Heliyon 10 (2024) e24080

Contents lists available at ScienceDirect

Heliyon

journal homepage: www.cell.com/heliyon

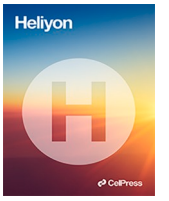

Research article

Anaerobic co-digestion of human excreta, food leftovers and kitchen residue: 1 ternary mixture design, synergistic effects and RSM approach

Blissbern Appiagyei Osei-Owusu [a,*], Richard Arthur [b], Martina Francisca Baidoo [c], Sampson Oduro-Kwarteng [d], Andrew N. Amenaghawon [e]

[a] *Regional Water and Environmental Sanitation Centre, Kumasi. Department of Civil Engineering, College of Engineering Kwame Nkrumah University of Science and Technology, UPO, Kumasi, Ghana*
[b] *Department of Energy Systems Engineering, Koforidua Technical University, Koforidua P.O. Box KF 981, Ghana*
[c] *Department of Chemical Engineering, Kwame Nkrumah University of Science and Technology, Kumasi, Ghana*
[d] *Regional Water and Environmental Sanitation Centre, Department of Civil Engineering, Kwame Nkrumah University of Science and Technology, UPO, Kumasi, Ghana*
[e] *Department of Chemical Engineering, University of Benin, Nigeria*

A R T I C L E I N F O

Keywords:
Anaerobic Co-Digestion
Biogas
Human Excreta
Food Waste
Biogas Potential
Mixture Design
Response Surface Method

A B S T R A C T

Anaerobic digestion of multiple substrates can generate more biogas while remaining stable, if positive synergistic effects are achieved. The type of co-digested substrates and the mixing ratio used, are the most important variables as each substrate has unique set of characteristics.

Optimizing the volume ratios by testing various substrate mixing ratios is a popular method for determining the best-performing ratio of substrate mixture. The ternary mixture design has reportedly been found to quicken the process of testing different mixing ratios with high accuracy without running several experiments. Therefore, a ternary mixture design and a response surface approach are used in this work to ascertain the relationship between substrate mix and responses (biogas yield, methane yield, and synergy). The findings of the experiment revealed that R9 comprising 78.8 % human excreta, 11.8 % food leftovers and 9.4 % kitchen residue, had the highest methane production of 764.79 $mLCH_4/gVS$ and a synergistic index of 3.26. Additionally, the 3D response surface plots from the response surface model showed important and shared interactions between Human Excreta, (HE), Food Leftovers (FLO), and Kitchen Residue (KR). HE and KR had a similar positive synergistic effect on biogas yield, methane yield, and synergy, which was not the case for FLO. The response surface plots showed that the predicted responses (methane yield, biogas yield and synergy) increased with increasing HE and KR fractions and decreased with increasing FLO fractions in the substrate mixtures.

* Corresponding author.
E-mail addresses: blissbernowusupeprah@gmail.com, bowusupeprah@st.knust.edu.gh (B.A. Osei-Owusu), richard.arthur@ktu.edu.gh (R. Arthur), mfbaidoo.coe@knust.edu.gh (M.F. Baidoo), sokwarteng@gmail.com, sodurokwarteng.coe@knust.edu.gh (S. Oduro-Kwarteng), andrew.amenaghawon@uniben.edu (A.N. Amenaghawon).

https://doi.org/10.1016/j.heliyon.2024.e24080
Received 5 August 2023; Received in revised form 31 October 2023; Accepted 3 January 2024
Available online 11 January 2024
2405-8440/© 2024 Published by Elsevier Ltd. This is an open access article under the CC BY-NC-ND license (http://creativecommons.org/licenses/by-nc-nd/4.0/).

1. Introduction

Human excreta and food waste are considered to be readily available human-generated waste that could be used for the production of biogas in households [1]. It is estimated that one-third of the world's population, approximately 2.4 billion urban dwellers, rely on onsite sanitation system installations such as public latrines and septic tanks [2]. In Ghana, about 58 % of the entire population rely on cesspit and Kumasi Ventilated Improved Pit (KVIP) latrines [2]. Furthermore, Arthur et al. [3] has reported that 38.6 % of rural dwellers in Ghana use flush and non-flush toilet facilities. Unfortunately, most of the liquid waste are disposed of untreated and indiscriminately into drainage ditches and open urban spaces [4]. Very few human excrement treatment facilities are available to treat the volumes of liquid waste generated, thus exacerbating the problem [5]. Also, several studies indicate that 55–80 % of municipal solid waste from developing countries are generated from households [6]. In Ghana, 8389 tonnes (constituting about 66 % of total household waste) of household organic wastes are reported to be generated per day in a study conducted by Miezah et al. [7].

Waste management, therefore, has become a major bottleneck for Ghana's economy, considering the large volumes of solid and liquid waste generated. The amount of waste produced in Ghana can most likely generate revenue for the government through recycling and energy generation. However, the country spends vast amount of money on solid waste management [8]. In an effort to address the problem of waste management, the government of Ghana put in place an Environmental Sanitation Policy in 1999 and revised in September 2010. The policy focuses on the provision of sites by the district assemblies for treatment and disposal of wastes (landfills, composting facilities, waste stabilization ponds, trickling filters, septage treatment plants, etc.) in order not to create health hazards and aesthetic problems. However, the policy does not provide much information on waste to energy strategies. A review of the environmental sanitation policy of Ghana have depicted a general reluctance by the district assemblies and the private sector to invest directly in to waste infrastructure due to the lack of enforcement of national policies and the general lack of co-ordination in the implementation of waste management programmes. The main focus of waste management has therefore been landfilling. Hence, it is imperative that Ghana looks into environmentally sustainable and financially viable solutions.

Anaerobic digestion (AD) has been regarded as an appealing method for treating high-strength organic wastes and generating bioenergy in the form of biogas, mostly CH_4 and CO_2 [9]. Over the years, decentralized AD treatment has been widely recognized as a viable waste management strategy [10]. The idea of decentralized treatments was first focused on the separation of grey (from the sink, shower, and laundry) and black (containing feaces and urine) water, which were subsequently treated and recycled on-site [11]. Currently, source-separable waste streams like food waste are included in decentralized treatments. According to Kyere et al. [10], a decentralized treatment system that incorporates AD may offer a cheap supply of energy for on-site use.

Different feedstocks, influenced by the uniqueness of locations, can be used to generate biogas [12]. However, many of these feedstocks cannot solely produce the desired biogas yield due to their physico-chemical characteristics [1]. As a result, multiple feedstocks are co-digested to produce biogas with the characteristics of the feedstock used highly influencing the biogas yields [13]. Khoufi et al. [14] and Kafle et al. [15] state that anaerobic co-digestion can maintain process stability with a higher rate of biogas production if substrates synergize. The two most important factors in this situation are the types of anaerobically co-digested feedstocks and the mixing ratios used [16]. The percentage of co-digested substrates that are mixed together affects the synergic activity of anaerobic co-digestion, as different substrates have different properties [17,18].

Selecting a suitable co-substrate and at the right mixing ratio is thus critical to improve biogas production due to the presence of

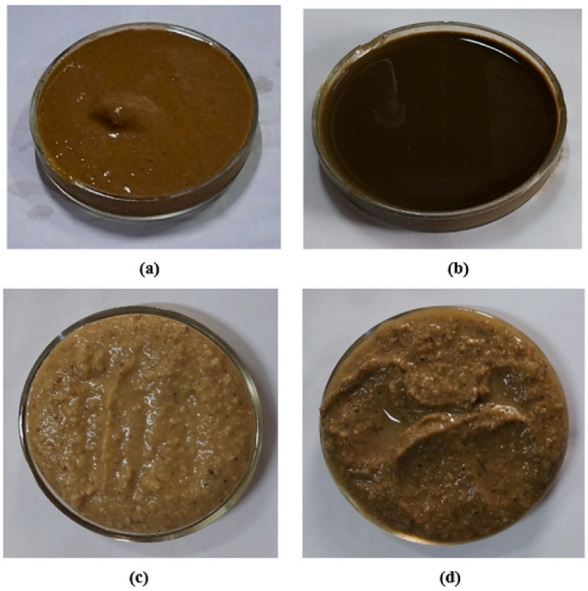

Fig. 1. Homogenized (a) human excreta (b) inoculum (c) food leftovers (d) kitchen residue.

native trace elements or sufficient buffer capacity [19]. Hence, the mixture of different substrates is a strategy to increase the performance of a digester in order to ensure an optimal feedstock composition and enhanced biogas production [20]. According to Andriamanohiarisoamanana et al. [21] and Andriamanohiarisoamanana et al. [22], investigations using the same feedstock and the same mixing ratio have reported conflicting results regarding synergic or antagonistic effects. It has been challenging to assess whether or not a particular waste stream can have synergistic benefits when digested together and, more significantly, to establish the best mixing ratios, due to these variances [23,24]. This phenomenon makes the setting or location where feedstocks are taken very important. Consequently, Hagos et al. [25] suggested investigating local or indigenous feedstocks, such as food waste and human excreta, due to the variation in composition across different settings.

The goal of the current study is therefore to examine the possibilities for using AD in the onsite treatment of human excreta (HE), food leftovers (FLO), and kitchen residues (KR). A reference biochemical methane potential (BMP) test, which could ultimately reveal methane yields of these wastes has been demonstrated in this study [26–30]. In addition, various mixing ratios are considered in order to investigate the impact of various substrate properties and compositions on methanogenic performance. Also, the minimal effective ratios of FLO and KR are determined in substrate mixture because there is competition for food waste to be used as animal feed [31]. The effect of mixing ratios on biogas yield, methane yield and synergy index are modelled and described using response surface plots. Although the use of food waste for biogas production has been extensively studied [32], information on the use of the combination of the different types of food waste described in this study and human excreta are not available. Also, this is a unique study, in that no data has been reported on the optimum mixing ratios for the co-digestion of HE, FLO and KR using a mixture design in the Ghanaian context. The results of this study will serve as a guide for the setup and operation of co-digestion systems for the on-site treatment of household generated waste.

2. Materials and methods

2.1. Feedstock and inoculum collection and preparation

Fresh HE (Fig. 1 a) was collected from a Kumasi Ventilated-Improved Pit (KVIP) at Ayeduase, a suburb in Kumasi, Ghana. Fresh cow dung was collected from the animal farm of the Department of Agriculture, KNUST. Anaerobically mono-digested cow dung (Fig. 1 b) with a pH of 7.8 and alkalinity of 8150 mg $CaCO_3$/L, was used as inoculum. The inoculum was degassed for two weeks under mesophilic condition (30 °C) until no gas production prior to use. The total solids (TS) and volatile solids (VS) of the inoculum were 3.82 ± 0.11 % and 79.10 ± 1.27 %, respectively. FLO and KR were also collected from households of staff and the canteen of a Senior High School in Kumasi, Ghana. FLO (Fig. 1 c) was mainly composed of milled rice, cassava, fufu, kenkey, yam, egg, fish, gari, beans, bread, banku, kontomire (cocoyam leaves) and some vegetable sauce. These are very common foods eaten in most households in Ghana. KR (Fig. 1 d), on the other hand, comprised of milled cassava peels, yam peels, cocoyam peels, plantain peels, lettuce residue, cucumber residue, tomato residue, carrot residue, garden eggs residue, avocado peels, banana peels, mango peels, orange peels, pineapple peels, onion peels, pawpaw peels and watermelon peels. FLO and KR were manually sorted to remove non-biodegradable fractions such as polyethene bags before organic fractions were shredded into smaller pieces, blended and homogenized into a slurry to maintain a particle size below 3 mm using a household food grinder and 3 mm sieve (Fig. 1). Samples were frozen at a temperature of −20 °C before use. The frozen samples were allowed to thaw at a temperature of 4 °C and used within a day to prevent biological decomposition.

Table 1
Experimental conditions for the BMP tests.

Ratio (HE: FLO:KR)[a]	HE (g)[b]	FLO (g)[b]	KR (g)[b]	Inoculum (g)[b]	Cellulose (g)[c]	C/N Ratio[e]
R1 (100:0:0)	75.00	0.00	0.00	233.00	0.00	11.79
R2 (0:100:0)	0.00	32.00	0.00	233.00	0.00	28.84
R3 (0:0:100)	0.00	0.00	84.00	233.00	0.00	20.36
R4 (0:50:50)	0.00	16.00	42.00	233.00	0.00	27.85
R5 (50:50:0)	37.00	16.00	0.00	233.00	0.00	15.45
R6 (50:0:50)	37.00	0.00	42.00	233.00	0.00	12.92
R7 (66.7:33.3:0)	50.00	11.00	0.00	233.00	0.00	11.89
R8 (66.7:0:33.3)	50.00	0.00	28.00	233.00	0.00	12.44
R9 (78.8:11.8:9.4)	59.00	4.00	8.00	233.00	0.00	23.98
R10 (54.7:21.8:23.5)	41.00	7.10	20.00	233.00	0.00	22.53
R11 (32.1:25.2:42.7)	24.00	8.00	36.00	233.00	0.00	17.10
R12 (0:33.1:66.9)	0.00	11.00	56.00	233.00	0.00	13.51
R13 (33.3:66.7:0)	25.00	22.00	0.00	233.00	0.00	23.27
R14 (16.7:16.6:66.7)	12.00	5.00	56.00	233.00	0.00	26.27
R15 (33.4:33.3:33.3)	25.00	11.00	28.00	233.00	0.00	15.21
R16 (16.7:66.7:16.6)	12.00	22.00	14.00	233.00	0.00	23.63
Blank[d]	0.00	0.00	0.00	233.00	0.00	22.88
Positive Control[e]	0.00	0.00	0.00	233.00	7.00	21.89

a: VS basis, b: Wet − weight basis, c: Dry − weight basis, d: Only inoculum, e: Pure cellulose and inoculum.

2.2. Analytical methods

The physical and chemical compositions of the feedstocks (HE, FLO, and KR) were evaluated before and after digestion by using standard procedure [33]. The pH was analyzed using a digital Hanner H1 98,136 pH meter. The TS and VS were analyzed using APHA methods 2540 B and APHA method 2540 E, respectively [33]. Total nitrogen was calculated following the Kjeldahl method [34], and the total amount of sulfur was determined using the spectrophotometer method [35]. Hydrogen was determined using titrimetric method [36] and organic carbon by Walkley–Black wet oxidation method [37,38]. The oxygen content was calculated as the positive difference between 100 and the sum of C, H, N, S, and ash content (AC) [12]. The C/N ratios of the samples was calculated by dividing the measured value of C and N [39]. Also, the alkalinity was determined according to the APHA method 2320 B using potentiometric titration [33]. VFA was determined titrimetrically [40–42]. PerkinElmer's NexION 2000 ICP-MS was used to detect the amounts of nickel (Ni), molybdenum (Mo), zinc (Zn) and iron (Fe) in the feedstocks. All results are reported as the mean ± standard deviation.

2.3. Formulation of substrate-mix using mixture design

A no-block, randomized ternary mixture experimental design with three variables, serving as mixture components, was adopted in this study to formulate the substrate mix from HE, FLO and KR. Sixteen (16) substrate mixtures with different mixing ratios (VS basis) of HE, FLO and KR were generated. The 'Design Expert' software version 13 (Stat-Ease, Minneapolis, MN, USA) was used to generate the experimental matrix. The different mix ratios of HE, FLO and KR in the substrate mixtures (from 0 to 100 %) (Table 1) were used as independent variables (input factors) to estimate the responses of biogas yield, methane yield and synergy. Equations (1) and (2) show the relationship between the components of the mixture which also represent factors of the design.

$$0 \leq HE, FLO, KR \leq 100 \quad \text{(Equation 1)}$$

$$HE + FLO + KR = 100 \quad \text{(Equation 2)}$$

For each of the runs (*Ri*), there were three bottles (triplicates) that were used. Ri_a, Ri_b and Ri_c, where "*i*" starts from 1 to 16 (Table 1).

2.4. Theoretical bio-methane potential (BMP_{TH})

The empirical relationship between the components of the feedstocks were determined using a modified Buswell equation by Boyle [43], as shown in Equation (3).

$$C_aH_bO_cN_dS_e + \left(a - \frac{b}{4} - \frac{c}{2} + \frac{3d}{4} + \frac{e}{2}\right) \times H_2O \rightarrow \left(\frac{a}{2} - \frac{b}{8} + \frac{c}{4} + \frac{3d}{8} + \frac{e}{4}\right) \times CO_2 + \left(\frac{a}{2} + \frac{b}{8} - \frac{c}{4} - \frac{3d}{8} - \frac{e}{4}\right) \times CH_4 + d \times NH_3 + e \times H_2S \quad \text{(Equation 3)}$$

The theoretical methane yield was estimated using Equation (4) [44–47].

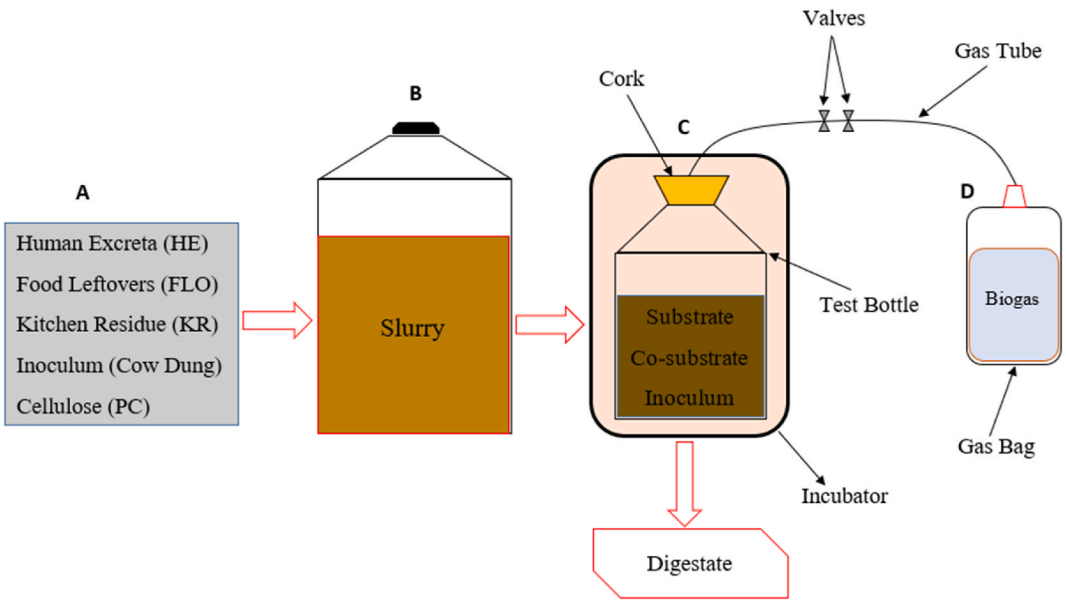

Fig. 2. Schematic diagram of BMP Setup.

$$BMP_{TH} = \frac{\left\lfloor \left(\frac{a}{2}\right) + \left(\frac{b}{8}\right) - \left(\frac{c}{4}\right) - \left(\frac{3d}{8}\right) - \left(\frac{e}{4}\right) \right\rfloor . 22400}{12a + b + 16c + 14d + 32e} \quad \text{(Equation 4)}$$

2.5. Biochemical methane potential (BMP) test

BMP tests of the different mixtures were carried out in 500 mL bottles with a working capacity of 300 mL. The schematic diagram of the BMP test is shown in Fig. 2.

An amount of 233 g of the inoculum and 7 g VS of a substrate combination were transferred into each bottle. A 1:1 inoculum to substrate ratio (ISR) (VS basis) was adhered to Ref. [48]. In total, 18 BMP runs (sixteen runs with the substrate mixtures (Table 1), one with the inoculum-only control and one run with a positive control of pure cellulose) were carried out in triplicates making 54 trials. The BMP bottles were tightly sealed (Fig. 3), incubated at (30 °C), manually and gently shaken daily for 61 days. Biogas production and composition were monitored on a daily basis. The generated biogas was collected in gas bags and measured through downward water displacement technique using an inverted glass chamber of 1000 mL capacity [26]. The measured biogas was corrected to standard conditions of 0 °C and 1 atm. Biogas composition was also determined with a portable Biogas 5000, Geotech UK) analyzer. VDI.4630 [49] assumes a substrate usage of 5 % during the fermentative stage and 3 % during the methanogenic stage, representing a total microbial biomass utilization of 8 % over the entire process. In this study, 8 % was used for specific methane yield correction.

2.6. Biodegradability (BD)

The extent of anaerobic biodegradability, BD, was calculated by dividing experimental methane yield (BMP_{exp}) by the theoretical methane potential (BMP_o) according to Equation (5) [50].

$$BD(\%) = \frac{BMP_{exp}}{BMP_o} \times 100 \quad \text{Equation (5)}$$

2.7. Synergy

Synergy index (SI) was determined as the ratio of methane yield of the co-digestion substrates ($M_{i,n}$) to the weighted average based upon VS content (%VS) of the methane yield of individual substrate ($M_{o\ i,n}$). This was calculated according to Equation (6) [51,52].

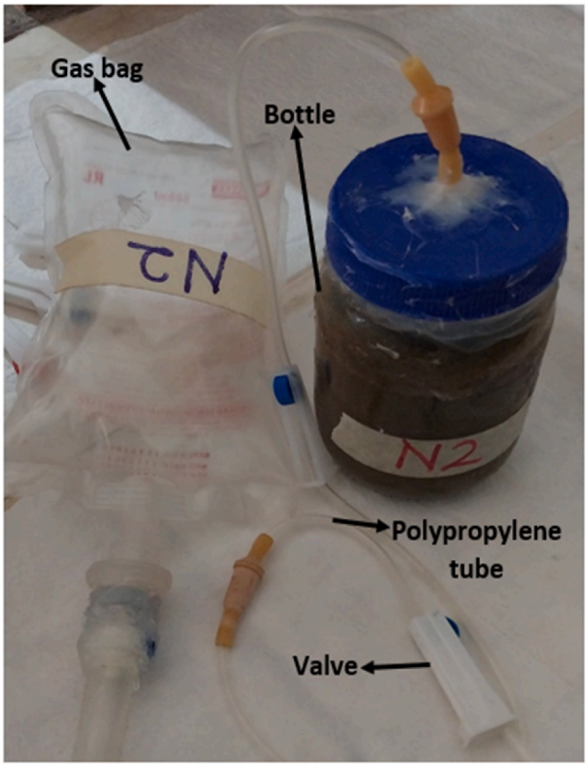

Fig. 3. Setup design for batch experiment.

$$SI = \frac{M_{i,n}}{M_{oi,n}} = \frac{M_{i,n}}{\sum_i^n \%VS_i M_{o,i}} \quad \text{Equation (6)}$$

where subscripts '*i*' through '*n*' denote the co-digested substrates and $\sum_i^n \%VS_i = 1$. An SI greater than one (>1) implies a synergistic impact, while an SI less than one (<1) indicates an antagonistic effect.

2.8. Response surface method (RSM) modelling

A sequential process of experimental data collection, polynomial equation construction, and model suitability assessment was used for RSM modelling. This was done through multiple regression analysis in order to assess the relationship between mixture components and the responses of biogas yield, methane yield and synergy. Increasing polynomials were fitted to the experimental data to model the response surfaces [53]. Anova and performance assessment results for the modelling, parity as well as 3D response surface plots were generated to show the effect of the interaction between input variables and the responses.

2.9. Statistical analysis

Samples were analyzed in triplicates and the results reported as the mean value ± standard deviation (SD). One-way analysis of variance (ANOVA) was then used to test the statistical significance of different digesters. Also, Tukey's honestly significant difference (HSD) test was used for the pairwise comparison of the mean biomethane composition obtained during co-digestion using Minitab v.19 software. ($p < 0.05$) was used as threshold for statistical significance.

3. Results and discussion

3.1. Feedstock characteristics

Table 2 provides information on the properties of the feedstocks (HE, FLO, and KR) employed in this study. The TS concentrations for HE, FLO, and KR were 11.34 ± 0.14, 25.80 ± 0.32 and 9.44 ± 0.00 %, respectively, while the VS contents were 82.81 ± 0.84, 83.99 ± 0.61 and 88.10 ± 0.37 %, respectively. These values are similar to what is reported by Appiagyei Osei-Owusu et al. [1]. According to Capson-Tojo et al. [54] and Li et al. [55], feedstocks with high VS and VS/TS values (Table 2) may contain organic materials that are highly biodegradable. KR, such as leftover fruits and vegetables, has a high moisture content, contributing to the low TS of KR. Neves et al. [56] have reported that majority of fruit and vegetable wastes contain high levels of volatile solids and easily biodegradable organic matter, but they lack total solids. In most cases, they hydrolyze quickly, producing acids that decrease the pH and limit the growth of methanogens [57]. While the pH values of FLO (5.0 ± 0.1) and KR (5.3 ± 0.1) were in the acidic range, that of HE (7.1 ± 0.1) was almost neutral. The presence of carbohydrates-containing food components, which can be converted to monosaccharides and then volatile fatty acids (VFAs) during the AD process, may be the reason for the low pH and buffer capacity of FLO and KR that was observed [58].

The C/N ratios of HE, FLO and KR, respectively, were 8.36 ± 0.01, 32.59 ± 0.13 and 29.34 ± 0.44 based on the elemental compositions. The AD process is often more stable at a C/N ratio of 20–30, with most of the carbon content being easily degradable [59–61]. HE in this study has a low C/N ratio, consistent with the 12.0 reported by Singh et al. [62]. However, the C/N ratios of FLO and KR are within the 20 to 30 range that Scherer et al. [44] proposed for anaerobic digestion. In order to improve the AD process, feedstocks with low C/N ratios should be combined with feedstocks with high C/N ratios for better anaerobic digestion performance [63].

3.2. Daily and cumulative methane yields of anaerobic digestion studies

Methane yield profiles varied between the 16-substrate mixing ratios. These variations were more pronounced throughout the study, especially during the first two weeks of incubation (Fig. 4). This was unsurprising as there were different combinations of

Table 2
Physicochemical Characteristics of Substrates [n = 3; mean (standard deviation)].

Parameter	HE	FLO	KR
TS (%)	11.34 (0.14)	25.80 (0.32)	9.44 (0.00)
VS (% TS)	82.81 (0.84)	83.99 (0.61)	88.10 (0.37)
VS/TS	0.83 (0.001)	0.84 (0.001)	0.88 (0.001)
pH	7.1 (0.1)	5.0 (0.1)	5.3 (0.1)
C (%)	61.22 (0.02)	41.16 (0.01)	38.10 (0.01)
N (%)	7.32 (0.02)	1.26 (0.01)	1.30 (0.02)
H (%)	9.02 (0.02)	9.52 (0.01)	8.52 (0.01)
O (%)	12.25 (0.01)	45.66 (0.01)	43.72 (0.01)
S (%)	0.200 (0.00)	0.135 (0.00)	0.031 (0.00)
C/N	8.36 (0.01)	32.59 (0.13)	29.34 (0.44)

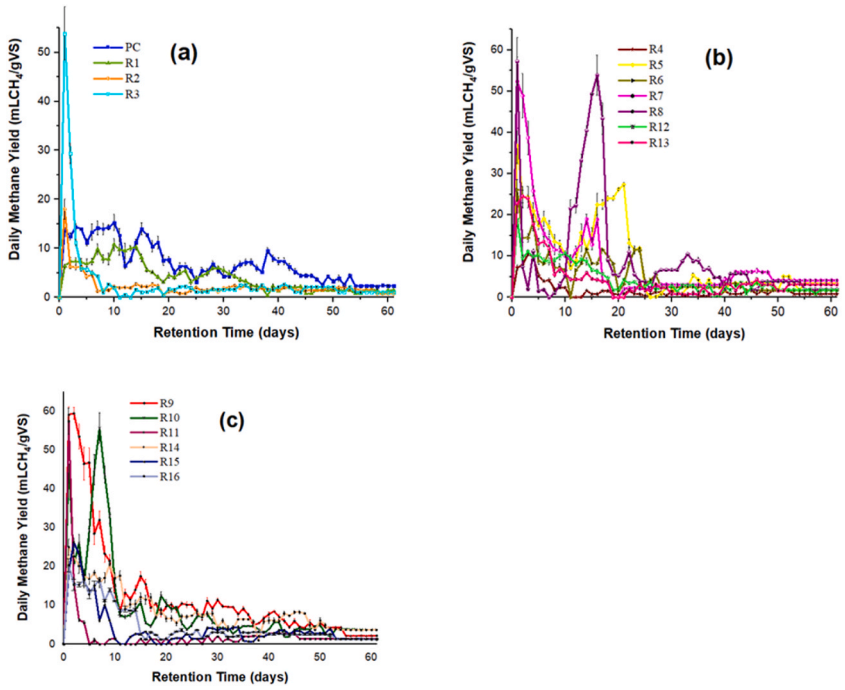

Fig. 4. Effects of different mixing ratios on daily methane yields: (a) monodigestion, (b) co-digestion, and (c) tri-digestion (mean ± S. D; n = 3) 90 % of measurements have RSD of less than 5 %.

feedstocks in the bottles. Generally, the daily methane yield increased to a peak and then drastically decreased in the first ten to fifteen days in all the mono digestion tests (Fig. 4a) [44]. The co-digestion and tri-digestion experiments also revealed a consistent pattern in the daily methane output, which peaked at high levels before gradually declining from days 30–35 to essentially no methane production (Fig. 4b and c). Fig. 4 displays the daily methane yield from the studies of the mono, co-, and tri-digestion AD tests. On the first day, the daily methane production ranged from 6.39 to 59.16 mL CH_4/gVS, demonstrating a rapid startup of the process. HE, FLO, and KR contained substantial amounts of components such as carbohydrates that were simple to digest and their conversion could happen extremely quickly. Fig. 4a demonstrates that on day 3, following the first peak, the biogas yield in the mono-digestion of FLO and KR significantly dropped. This was most likely caused by a drop in system pH brought on by the conversion of organic matter in the FLO and KR to VFA, whose build-up might have prevented biogas synthesis [64]. As illustrated in Fig. 4b, the co-digestion of HE: FLO (R5, R7, R13) and HE: KR (R6, R8) similarly showed possible minor acidification with a decrease in biogas on days 3 and 4. However, the acidification of the co-digestion test was relatively mitigated compared with the mono-digestion of individual feedstock because of the alkalinity levels (3437.50–5975.00 mg $CaCO_3$/L) of all treatments and the buffer capacity from HE. In contrast, negligible acidification was observed in the tri-digestion tests (Fig. 4c).

Although R5, R7, R8, R9, and R10, hydrolyzed quickly, the process was remarkably steady compared to the other mix ratios with less or no HE (Fig. 4). This was evident by comparing the initial and final alkalinity (4537.00–6587.50 mg $CaCO_3$/L and 1362.50–2987.50 mg $CaCO_3$/L, respectively), initial and final pH (7.1–7.9 and 6.1–6.6, respectively) and initial and final VFA concentrations (2309.79–3555.38 mg/L and 1082.33–1680.94 mg/L, respectively) as shown in Table 3. Additionally, the daily methane productions from the HE-added reactors R5, R7, R8, R9, and R10 were higher than those from reactors (R2, R4 and R12) without HE over the first seven days (Fig. 4b and c). Independent of the mixing ratios, the peak values of R5, R7, R8, R9, and R10 were observed earlier. This held true, in particular, for feedstocks containing 50 % or more HE (R5, R7, R8, R9 and R10, Fig. 4b and c). The use of readily biodegradable materials such as carbohydrates from FLO and KR may be the reason why the peak values of daily methane production from the HE-added reactors (R5, R7, R8, R9 and R10) were observed to experience a gradual reduction, while reactors with no HE (R2, R4, R12) sharply declined after the first few days. As seen in Fig. 4, R9 recorded the highest daily methane production of all the reactors, peaking at 59.51 mLCH_4/gVS whereas R5, R7, R8 and R10 peaked at 36.78, 52.33, 57.25 and 55.71 mLCH_4/gVS respectively. Further, the reactors with high HE ratios produced more methane daily. This finding suggests that increasing the amount of HE to FLO and KR is advantageous for increasing methane generation, probably because of the sufficient alkalinity and nearly neutral pH of HE. Additionally, this could also be associated with the presence of native nutrients or trace elements in HE [65].

The cumulative methane yields from the mono-digestion of HE (R1), FLO (R2), KR (R3), and cellulose (positive control, PC) are 253.89, 135.27, 198.86, and 435.36 mLCH_4/gVS, respectively, as shown in Fig. 5 a. Also, the cumulative methane yields from the co-digestion and tri-digestion tests are shown (Fig. 5 b and c, Table 3). It was discovered that the mono-digestion tests for FLO and KR produced less methane than the mixed groups. This might be due to the high levels of VFA buildup [66] in FLO and KR (R2:4141.89 mg/L and R3:3543.28 mg/L, respectively) as well as the lower levels of alkalinity in FLO (R2:1775.0 mg $CaCO_3$/L) and KR (R3:1900.0

Table 3
Biogas and Methane Yields, VFA, pH, Alkalinity, Biodegradability and VS Reduction for different mix ratios of HE, FLO and KR in AD Tests.

Parameter	R1	R2	R3	R4	R5	R6	R7	R8	R9	R10	R11	R12	R13	R14	R15	R16	PositiveControl
Specific biogas yield (mL/g VS added)	453.37	375.76	473.47	254.61	802.59	527.82	782.97	887.27	1167.62	881.33	322.75	611.12	482.27	990.54	417.56	632.94	762.45
Methane Content (%)	56.00	36.00	42.00	40.00	67.90	59.90	63.20	64.60	65.50	67.60	48.50	42.70	56.70	53.10	59.00	46.00	57.10
Specific methane yield (mL/g VS added)	253.89	135.27	198.86	101.84	544.96	316.16	494.83	573.18	764.79	595.78	157.50	260.95	273.45	525.98	246.36	291.15	435.36
Specific methane yield correction with 8 %	274.20	146.09	214.77	109.99	588.56	341.45	534.42	619.03	825.97	643.44	170.10	281.83	295.33	568.06	266.07	314.44	470.19
Theoretical methane potential (mL/g VS added)	461.12	833.60	745.18	727.27	657.61	586.04	602.69	642.59	851.83	689.99	609.60	646.77	565.84	659.05	773.17	774.99	551.35
Biodegradability (%)	55.06	16.23	26.69	14.00	82.87	53.95	82.10	89.19	89.78	86.18	25.84	40.35	48.33	79.81	31.86	37.57	78.96
Corrected Biodegradability (%)	59.46	17.53	28.82	15.12	89.57	58.26	88.67	96.10	96.91	93.25	27.90	43.57	52.19	86.19	34.41	40.57	85.28
VS reduction (%)	47.81	41.79	46.94	36.71	60.72	50.69	59.68	62.67	67.62	63.49	38.43	51.76	47.19	66.79	43.75	53.08	57.99
Initial pH	7.1	6.3	6.1	6.0	7.1	7.3	7.4	7.5	7.9	7.4	6.7	6.7	6.6	6.8	6.7	7.0	7.3
Final pH	6.3	5.0	5.3	4.9	6.1	6.2	6.6	6.2	6.1	6.3	5.4	6.3	6.0	6.3	5.2	5.6	6.7
Initial Alkalinity (mg/L)	7432.50	2662.50	2525.00	1712.50	4537.50	5537.50	5887.50	5975.00	6587.50	6412.50	1512.50	1925.00	3437.50	3850.00	3537.50	1687.50	3512.50
Final Alkalinity (mg/L)	3950.00	1775.00	1900.00	1287.50	1362.50	2087.50	2825.00	2987.50	2700.00	1725.00	1275.00	1637.50	1437.50	1112.50	1625.00	1562.50	3100.00
Initial VFA (mg/L)	3652.12	4141.89	3543.28	3549.33	2956.77	1711.18	3507.00	3555.38	2890.25	2309.79	3537.24	3017.23	2920.49	3597.70	4147.94	4153.99	1747.46
Final VFA (mg/L)	2866.07	3567.47	2962.81	3005.14	1668.85	1064.19	1680.94	1674.90	1481.41	1082.33	2309.79	2932.58	1711.18	1106.52	3500.96	2902.35	1124.66

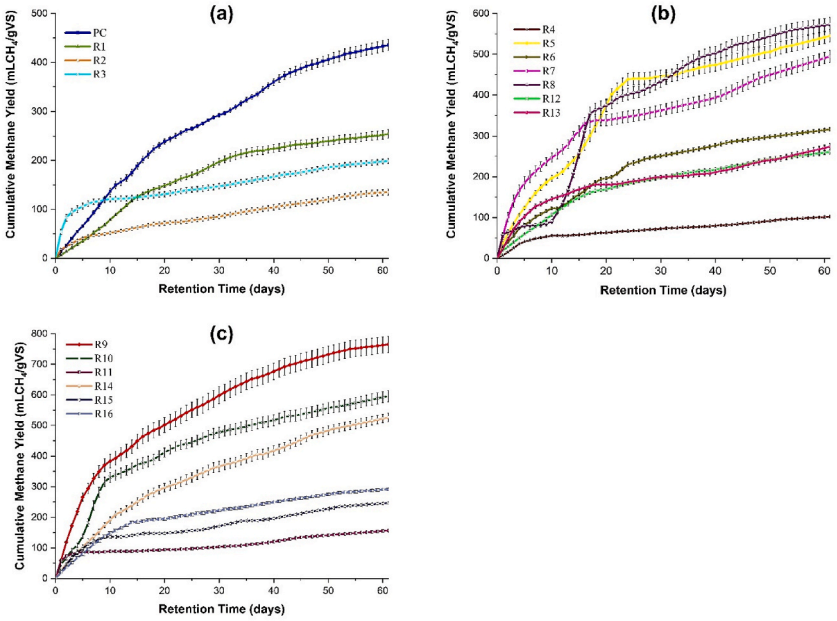

Fig. 5. Effects of different mixing ratios on cumulative methane yields: (a) monodigestion, (b) co-digestion, and (c) tri-digestion (mean ± S. D; n = 3) 90 % of measurements have RSD of less than 5 %.

mg $CaCO_3$/L) (Table .3). Filer et al. [26] recommends that alkalinity be kept at 3000 mg$CaCO_3$/L to maximize methane yield. As in the case of the daily yields, the substrate mixtures with HE percentages of 50 % or higher (R5 = 544.96 mLCH_4/gVS, R7 = 494.84, R8 = 573.18 mLCH_4/gVS, R9 = 764.79 mLCH_4/gVS, R10 = 595.78 mLCH_4/gVS) had higher cumulative methane production. The highest cumulative methane production was 764.79 mL CH_4/gVS, corresponding to the tri-digestion R9 of HE:FLO:KR (78.8:11.8:9.4), followed by R10 (595.78 mLCH_4/gVS), which were all having a greater amount of HE (>50 %). The cumulative methane output of R9 was 66.80 % higher than that obtained for the mono-digestion of HE (R1). This was presumably due to the fact that there were varieties of substrates available, which provided the different useful microbial population with enough native nutrients to promote the breakdown of substrates and increase biogas generation [67].

In comparison with the mono-digestion tests, the results demonstrated that the multiple substrates digestion (R9, R10, R14 and R15) had a superior capacity for buffering (alkalinity range of 3537.50–6587.50 mg $CaCO_3$/L) and was relatively stable for the production of biogas. Conversely, the rapid build-up of intermediates like VFAs with consequently low buffer capacity, may have caused the low methane levels of the mono-digestion test [68]. Singh et al. [62] reported increased daily biogas output for the co-digestion of human excreta, cow dung, and poultry litter as opposed to mono-digestion, further demonstrating the more reliable performance of the mixed feedstock digestion system. Despite variations in the rate of methane production and yield between all BMP operations, methane was produced continuously without any lag phase. This could be explained by the high percentage of inoculation (40 %) used in the BMP testing, which might have offered a significant number of active bacteria and a supply of nutrients for microbial development. Additionally, the biodegradable organic content of the substrate mixtures had a significant role in determining the effectiveness of co-digestion. For each of the tests (R1-R16), the mean values of methane content were reported (Table 3). A one-way ANOVA with a p-value of $p < 0.001$ revealed a statistically significant difference between the methane production from the tests (R1-R16). Therefore, different mixing ratios have different methane yields.

3.3. Effects of VS reduction, CN ratio, pH, alkalinity and VFA on methane yields

The initial and final VS contents for the mono-, co-, and tri-digested substrates revealed an overall decreasing tendency for all mix ratios. Table 3 displays the VS reduction values for all treatments from R1 to R16. The VS reduction trend was connected with the generation of methane. In this study, HE had a very low C/N ratio compared to FLO and KR. Similarly, Singh et al. [62] reports of lower C/N ratio for HE. Combining HE with carbon-rich organic wastes like FLO and KR improves nutrient balance and the C/N ratio [62]. Tri-digestion of R9 exhibited the highest biogas and methane yields, followed by R10 (Table 3). This can be partly traced to the C/N ratios of R9 (23.9) and R10 (22.5). Generally, a C/N ratio of 20–30 gives a more stable anaerobic digestion process [18,59,60]. It was found that co- and tri-digestion could maintain C/N ratios at ideal values due to the mixture of various substrates, which enhanced biogas production (Table 1). Combining HE with FLO and KR helped achieve the optimal C/N ratio, thereby improving digestion. A considerable amount of biogas and methane was also produced in the co-digestion treatments R5, containing high amounts of HE, even at the low C/N ratio of 15.45. This could be because HE is nutrient-rich and contains adequate amounts of native trace elements like Fe, Ni, Zn and Co essential for the growth of anaerobic bacteria [69].

On the other hand, low pH and buffer capacities were observed for FLO and KW. Li et al. [55] has reported a similar trend. Hence, mono-digestion of FLO and KR is not always desirable. Co-digestion of these substrates at certain optimum proportions may improve methane production performance. The initial and final pH and alkalinity values for all treatments are summarized in Table 3. Mixing feedstocks raised the pH of the mixtures containing FLO and KR relative to their individual pH values. This could be observed from Table 3 where combinations of FLO and KR with higher proportions of HE had high pH values at the start of digestion and vice versa. The initial pH values of R5, R7, R8, R9 and R10 were within the range of 7.1–7.9, while the pH values after digestion were within the range of 6.1–6.6 (Table 3). Hence, the observed pHs of the digesters (R5, R7, R8, R9 and R10) were within the acceptable range for anaerobic digestion [70]. In addition, the initial and final alkalinity of R5, R7, R8, R9 and R10 were within the ranges of 4537.5–6587.5 mg/L and 1362.5–2987.5 mg/L respectively. Due to the optimal pH values and the strong alkalinity providing a very good buffer for the bottles R5, R7, R8, R9 and R10, biogas and methane production were stable [44,71], obtaining a biodegradability range of 82.1–89.8 % (Table 3). On the other hand, treatments R2, R3, R4, R11 and R16 with very low initial alkalinity in the range of 1512.5–2662.5 mg/L and final pH in the range of 4.9–5.6, had very low biogas and methane yields and hence very low biodegradability values as expected (Table 3). This observation is consistent with the information in Table 3 and could be explained by the buildup of VFAs from the conversion of readily biodegradable components in the digestive media. Conversely, treatments with 50 % or more HE added like R9 and R10 were observed to ensure a stable AD system stability due to the low initial and final VFA values ranging between 2309.8 and 3555.4 mg/L and 1082.3–1680.9 mg/L respectively and this finding might provide an explanation for the best biogas yield, methane yield and biodegradability data recorded (Table 3). The VFA/Alkalinity ratios of 0.43 and 0.35 for R9 and R10 respectively is a confirmation of how stable the anaerobic digestion process was. According to Feng et al. [72], a VFA/Alkalinity ratio of 0.4 indicates stability of anaerobic digestion process.

3.4. Effect of native trace elements in substrate mixtures on methane yield

Trace elements that are often present in human-generated waste, such as iron (Fe), nickel (Ni), zinc (Zn) and molybdenum (Mo) [1], were studied to investigate their effect on methane yields of the different mixtures (R1-R16). All treatments contained Fe, Ni, Zn and Mo concentrations in the range 1.7150–8.5298, 0.0017–0.0530, 0.1552–0.5541 and 0.0067–0.0700 mg/L respectively (Table 4). Fe had all treatments outside the stimulatory concentration of <0.3 [73], with the highest and lowest concentrations for R16 (8.53 mg/L) and R3 (1.72 mg/L), respectively. Also, with stimulatory concentrations of $0.03 < Zn < 2$ and $0.03 < Ni < 27$ for Zn and Ni respectively, all treatments were within the stimulatory range [74,75]. The treatments with the highest Zn concentrations were R9 (0.554 mg/L) and R10 (0.414 mg/L), while the least concentrations were found in R1 (0.211 mg/L), R2 (0.200 mg/L) and R3 (0.210 mg/L) respectively (Fig. 6). Considering the important role of Zn for activating and maintaining enzyme activities of anaerobic microorganisms [76,77], they were possibly insufficient for stable and mono-digestion tests R1, R2 and R3.

It is therefore recommended that the concentrations of essential trace elements be properly adjusted by mixing HE, FLO and KR. Contrarily, R9 and R10 with the highest methane yields, were found to contain the highest concentrations of Zn. These results confirm the positive influence of Zn on enzymes such as coenzyme *M. methyltransferase*, involved in methanogenesis [78]. Similarly, optimum concentrations of Ni in R5 (0.043 mg/L), R7 (0.033 mg/L), R8 (0.027 mg/L), R9 (0.053 mg/L) and R10 (0.022 mg/L) significantly increased their methane yields (Fig. 7). Arthur et al. [78] reported an increase in the number of methanogens present in reactors containing nickel. The author also documented that nickel concentration of less than 0.1 mg/L improved the stability of the anaerobic digestion process because intermediary products were readily digested by methanogens [78]. Further, Schmidt et al. [79] reported a rapid accumulation of VFAs when Ni was depleted. The trace elements in bottles R7, R8 R9 and R10 with high methane yields are in the order Fe > Zn > Ni > Mo. Fermoso et al. [80] illustrated the fundamental role of these micro nutrients by demonstrating their interactions with microbe cells.

Overall, the elements in methanogens cells were in the following order Fe > Zn > Ni > Cu═Co═Mo > Mn. Also, Schönheit et al.

Table 4
Concentration of native trace elements in substrate mix.

Treatment	Mo (mg/L)	Zn (mg/L)	Fe (mg/L)	Ni (mg/L)
R1	0.0171	0.2108	2.8353	0.0029
R2	0.0144	0.1995	1.9148	0.0017
R3	0.0117	0.2074	1.7150	0.0025
R4	0.0127	0.2637	2.9204	0.0051
R5	0.0675	0.3080	4.3026	0.0427
R6	0.0085	0.2121	2.9789	0.0138
R7	0.0700	0.2547	3.3521	0.0326
R8	0.0124	0.3011	3.7329	0.0374
R9	0.0072	0.5541	3.8201	0.0530
R10	0.0083	0.4141	2.9879	0.0431
R11	0.0100	0.2155	7.6721	0.0050
R12	0.0077	0.2552	4.0839	0.0092
R13	0.0070	0.2309	2.5650	0.0032
R14	0.0067	0.2348	2.5491	0.0358
R15	0.0085	0.3010	3.0142	0.0018
R16	0.0103	0.2285	8.5298	0.0034

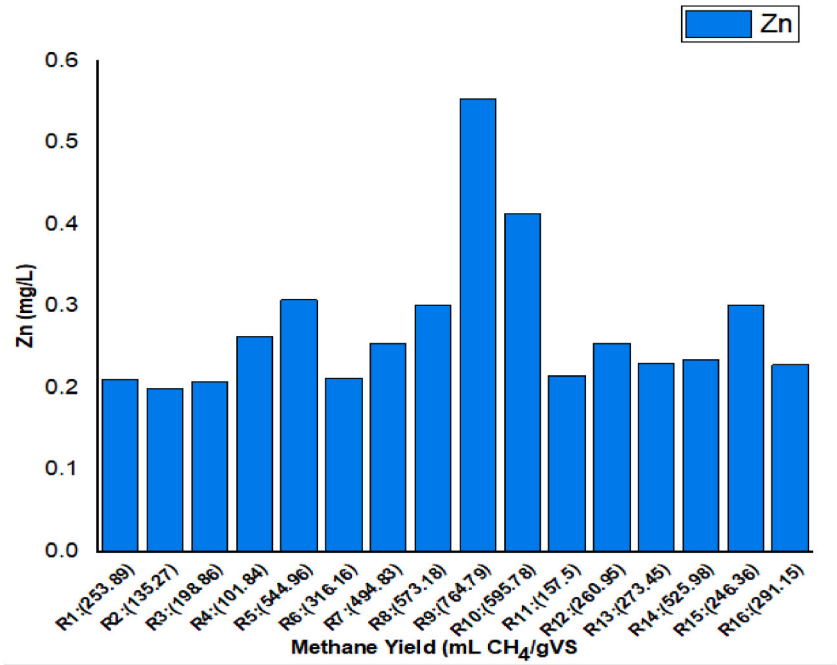

Fig. 6. Effect of zinc concentrations on methane yield.

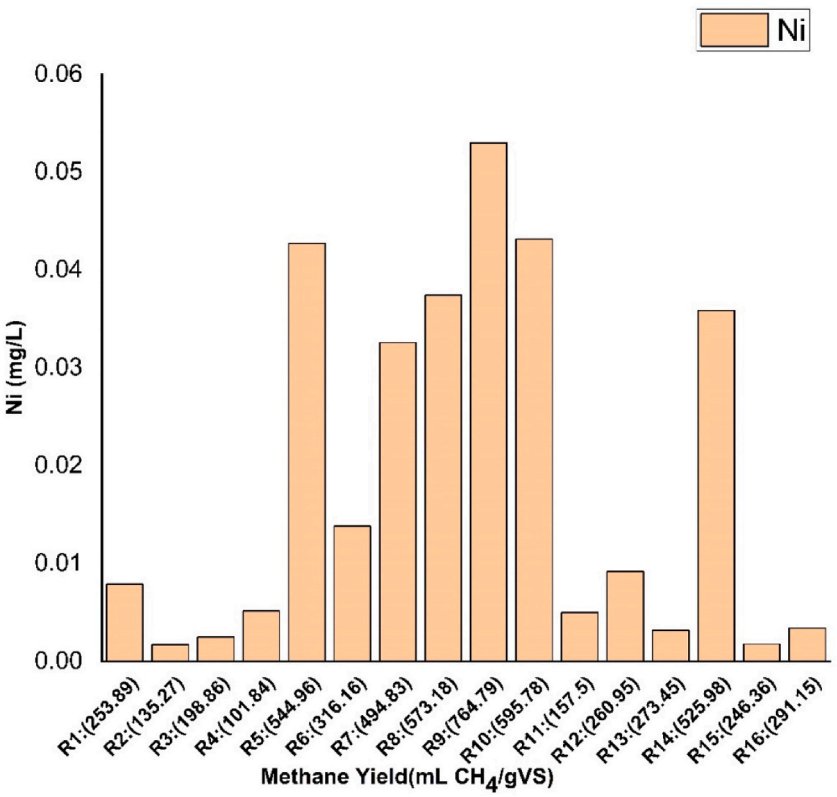

Fig. 7. Effect of nickel concentrations on methane yield.

[81] discovered that *Methanobacterium thermoautotrophicum* grew in response to trace elements of Fe > Ni > Co═Mo. As mentioned above, the trace elements supplied from the mixtures seemed to increase the process stability of anaerobic co- and tri-digestions. However, due to factors like C/N ratio, pH and alkalinity values of the individual co- and tri-digestion tests, some process upsets were observed in some treatments like R6 and R15 as indicated by VFA accumulation even though they had sufficient amounts of Zn and Ni.

3.5. Synergistic effects of Co- and tri-digestion tests

Fig. 8 compares the synergy index (SI) for multiple substrate digestion of HE, FLO and KR among the BMP runs. Also, the SI values for the co- and tri-digestion runs (Runs 4–16) ranging from 0.61 to 3.26 can be used to access how.

The individual mixtures affect the amount of methane generated. R5, R6, R7, R8, R9, R10, R12, R13, R14, R15,16 with SI values in the range 1.26–3.26 depicted stronger positive synergic effects. Additionally, R9 showed the highest SI value (3.26). The co- and tri-digestion runs containing an appropriate mix of FLO, and KR tended to produce more

Methane with higher HE percentages. The properties and ratios of the AD mixtures may have a bearing on the synergistic impact. These factors might have balanced the nutrients, promote microbial proliferation, boost buffer capacity, and dilute toxic substances during digestion. Wang et al. [82] have shown that the synergistic impact is caused by the addition of beneficial nutrients, which can improve biodegradability and enhance the metabolism of microorganisms. It can also be observed from Fig. 9 that bottles (R5, R6, R7, R8, R9 and R10) with initial alkalinity values of over 4500 mg/L and final alkalinity of about 2000 mg/L and above showed a positive synergistic effect. Conversely, R4 and R11 with initial alkalinity values around 2000 mg/L and final alkalinity around a 1000 mg/L exhibited an antagonistic effect with SI values of 0.61 and 0.78, respectively (Fig. 9). This is because R4 and R11 contained no or less amounts of HE. Also, the high amounts of KR (mainly composed of lignin-containing feed stock.

Like plantain peels, cassava peels, cocoyam peels and yam peels) in R4 and R11 might have led to the negative synergistic effects. Kim et al. [9], in their study of food waste, human feaces and toilet tissue, reported no obvious positive or negative synergic effects with reported SI values of 0.939–1.05. However, Ebner et al. [52] reported an SI value of 0.68 for the co-digestion of food waste and dairy manure, indicating a clear antagonistic effect. Conversely, Hou et al. [51] reported significantly positive synergic effects (1.03–1.24) for food waste, rice straw and bran.

3.6. Modelling of responses

Analysis of the experimental data revealed that quartic models [83] shown in Equations (7)–(9) were suitable for expressing biogas yield, methane yield and synergy as a function of the mixture components (Human Excreta-A, Food Leftovers-B and Kitchen Residue-C). The validity of the models was checked by plots of the model predicted values against the experimental (actual) values as

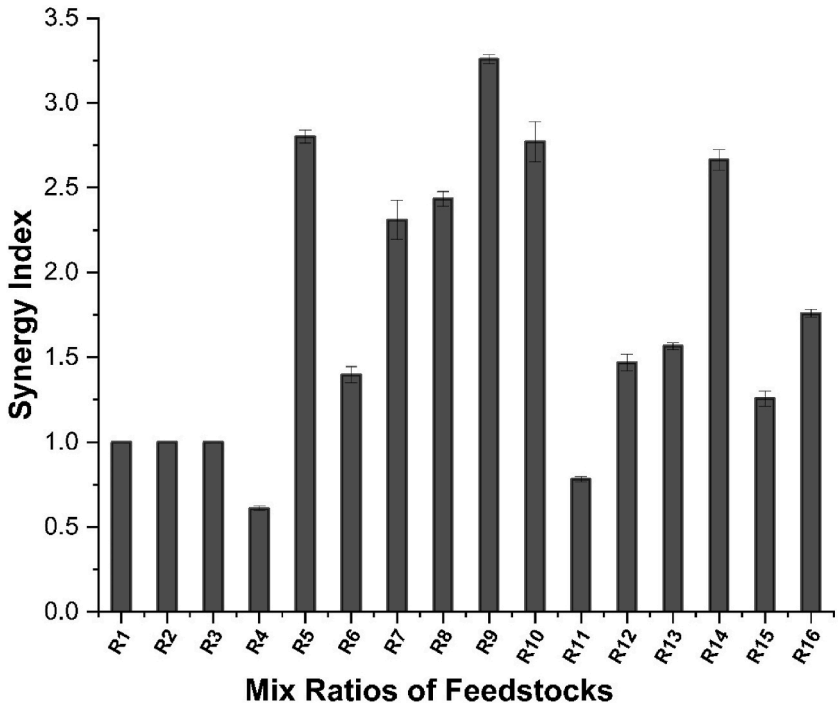

Fig. 8. Synergy index of substrate mix at different HE/FLO/KR ratios. SI > 1 indicates synergistic effect, and SI < 1 indicates antagonistic effect (mean ± S. D; n = 3).

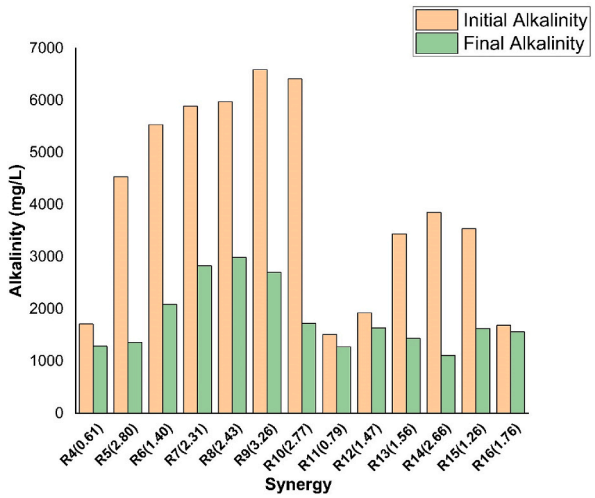

Fig. 9. Effect of alkalinity on synergy index of substrate mixtures.

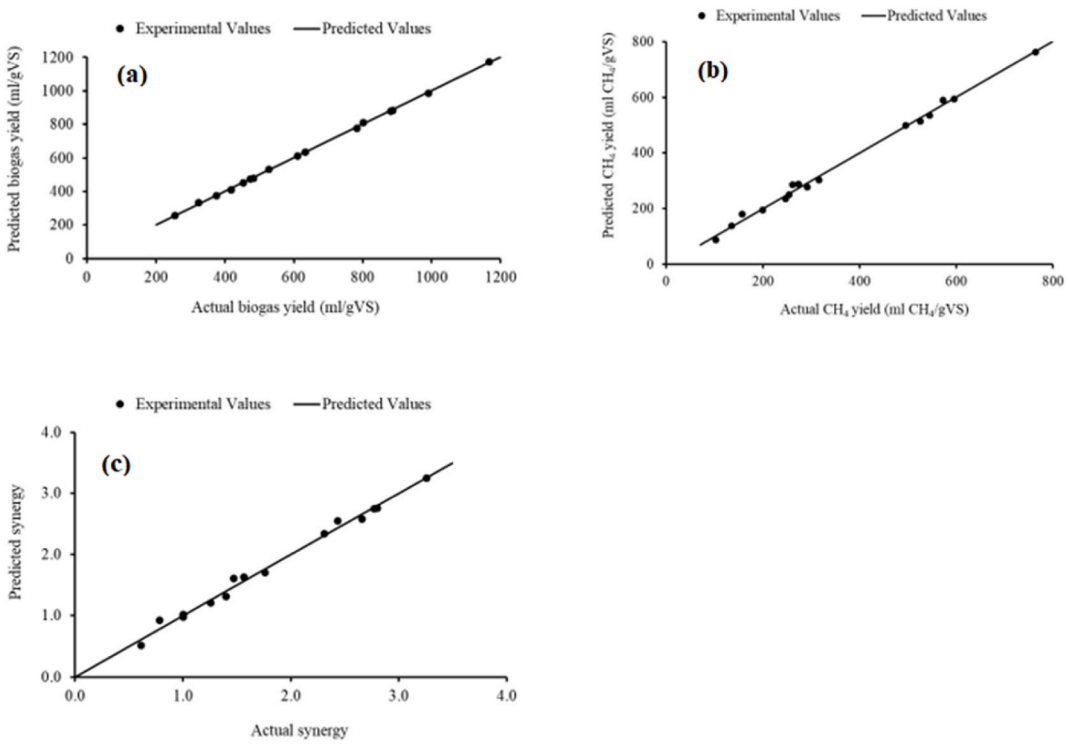

Fig. 10. Parity plots of experimental and predicted (a)biogas yield, (b) methane yield and (c) synergy as a function of the mixture components.

shown in Fig. 10. The plot of biogas yield (Fig. 10a) showed that the slope line passes exactly through all points while the plots of methane yield (Fig. 10b) and synergy (Fig. 10c) passes approximately through the data points. The relative similarity between the experimental observations and the model predictions indicates the validity, precision and good predictive capacity of the RSM model.

$$\textbf{\textit{Biogas Yield}} = 452.73A + 375.54B + 474.13C + 1587.49AB + 264.52AC - 680.02BC + 7387.14ABC + 1842.66AB(A-B) - 1139.33AC(A-C) + 10187.44A^2BC - 44978.31ABC^2 - 5628.27AB(A-B)^2 + 18180.83AC(A-C)^2 + 12644.33BC(B-C)^2 \quad \text{Equation (7)}$$

Table 5
ANOVA results for the RSM models of biogas yield, methane yield and synergy.

Parameter	Biogas Yield					Methane Yield					Synergy				
Source	Sum of Squares	df	Mean	F-value	p-value	Sum of Squares	df	Mean	F-value	p-value	Sum of Squares	df	Mean	F-value	p-value
Model	1.03E6	13	79583.31	431.81	0.00231	5.75E5	11	52259.87	81.14	0.00035	10.36	11	0.94	42.34	0.00126
Linear Mixture	218,353.15	2	109176.58	592.38	0.00169	203884.21	2	101942.11	158.27	0.00016	2.16	2	1.08	48.67	0.00156
AB	122,998.06	1	122998.06	667.38	0.00150	96561.44	1	96561.44	149.92	0.00026	2.57	1	2.57	115.53	0.00042
AC	3020.38	1	3020.38	16.39	0.05595	5180.83	1	5180.83	8.04	0.04705	0.08	1	0.08	3.81	0.12257
BC	20,604.35	1	20604.35	111.80	0.00883	4860.01	1	4860.01	7.55	0.05154	0.18	1	0.18	8.01	0.04735
ABC	1935.39	1	1935.39	10.50	0.08348	NA									
AB(A-B)	34,244.95	1	34244.95	185.81	0.00534	15820.60	1	15820.60	24.56	0.00773	0.27	1	0.27	12.29	0.02478
AC(A-C)	2193.77	1	2193.77	11.90	0.07472	NA									
A^2BC	1879.83	1	1879.83	10.20	0.08564	17402.08	1	17402.08	27.02	0.00653	0.42	1	0.42	18.95	0.01213
ABC^2	17178.31	1	17178.31	93.21	0.01056	47077.28	1	47077.28	73.09	0.00103	1.05	1	1.05	47.29	0.00234
$AB(A-B)^2$	23297.21	1	23297.21	126.41	0.00782	17484.53	1	17484.53	27.15	0.00647	0.54	1	0.54	24.19	0.00794
$AC(A-C)^2$	121,489.29	1	121489.29	659.19	0.00151	133044.11	1	133044.11	206.56	0.00014	2.66	1	2.66	119.72	0.00040
$BC(B–C)^2$	76420.15	1	76420.15	414.65	0.00240	37525.29	1	37525.29	58.26	0.00158	1.25	1	1.25	56.31	0.00169
Residual	368.60	2	184.30			2576.37	4	644.09			0.09	4	0.02		
Cor Total	1.04E6	15				5.77E5	15				10.45	15			
CV (%)	2.16					7.0817					8.4991				
Mean	629.00					358.3755					1.7546				
SD	13.58					25.3790					0.1491				
AP	72.31					30.7516					21.1644				

$$\textit{Methane Yield} = 250.47A + 138.25B + 196.17C + 1363.05AB + 318.22AC - 320.97BC + 1178.90ABAB(A-B) + 13479.78A^2BC - 22626.90ABC^2 - 4195.21AB(A-B)^2 + 11530.09AC(A-C)^2 + 7085.93BC(B-C)^2$$

Equation (8)

$$\textit{Synergy} = 0.97A + 1.02B + 0.99C + 7.03AB + 1.29AC - 1.94BC + 4.90AB(A-B) + 66.34A^2BC - 106.95ABC^2 - 23.27AB(A-B)^2 + 51.58AC(A-C)^2 + 40.93BC(B-C)^2$$

Equation (9)

The statistical significance of the RSM model was assessed by carrying out ANOVA, with results shown in Table 5. Model terms with p-values less than 5 % (0.05) are significant, while the reverse is also the case [83]. In this context, the biogas yield, methane yield and synergy models with p-values of 0.0023, 0.0004 and 0.0013, respectively, were significant (good in predicting the output responses) as they were characterized by p-values significantly less than 0.05. Also, the model F-values of 431.81, 81.14 and 42.34 for biogas yield, methane yield and synergy, respectively, showed that the model is significant implying that there is only a 0.23, 0.04 and 0.13 % chance that F-values this large could occur due to noise (Table 5). Hence the model is very good at predicting the responses.

Further, the Adequate Precision (AP) values of 72.31,30.75 and 21.16 for biogas yield, methane yield and synergy, respectively, indicate an adequate signal and the ability of the model to be used to navigate the design space (Table 5). This is because the measure of the signal-to-noise ratio is desirable when greater than 4 [84,85]. In addition, the linear terms representing the amount of HE (A), FLO (B) and KR (C) were all significant, indicating that varying the amount of feedstocks mixture components will have a significant influence on biogas yield (0.00169), methane yield (0.00016) and synergy (0.00156). There is therefore the need to test different amounts of household-generated waste in order to find the best ratios for a stable household biogas generation process.

However, the terms representing the interaction between HE and KR (AC and AC (A-C)) as well as HE, FLO and KR (ABC and A^2BC) in the biogas yield and synergy models were not significant. These terms were nonetheless, retained in the model to maintain model hierarchy (Table 5). The biogas yield, methane yield and synergy predicted by the RSM model were respectively characterized by small magnitudes of standard deviation (13.58, 25.38, and 0.15) compared to the mean value of 629.00, 358.38 and 1.75, indicating minimal dispersion of the data sets (Table 5). This was confirmed by the coefficient of variation, CV, values of 2.16, 7.08 and 8.50 %, respectively, for biogas yield, methane yield, and synergy. These CV values were low enough to indicate the precision and reliability of the data (Table 5).

RSM performance assessment for the biogas yield, methane yield, and synergy models was carried out using standard statistical metrics, as shown in Table 6. A good model is one that gives an R^2, adjusted R^2 and or predicted R^2 values approaching unity.

Le Man et al. [86] documented that a model is only adequate when R^2 values are not less than 0.75. Nonetheless, Koocheki et al. [87] stated that a high R^2 value does not necessarily imply a good regression model until there are similarly high values of adjusted R^2. Therefore, high R^2 and adjusted R^2 values can both be used to explain how adequate a model is to predict within the range of experimental values. That notwithstanding, the difference between R^2 and adjusted R^2 should not be more than 10 % [88]. The reported R^2 values in this study indicate that the quartic model was very accurate in predicting the biogas yield (0.999), methane yield (0.996), and synergy (0.992) as shown in Table 6. Although all models showed good predictive performance, as seen in their high R^2 values, the biogas yield model was relatively better in its prediction because it had the highest R^2 (0.999) value and a low error value (RMSE of 4.798). This was corroborated by the results in the parity plots presented in Fig. 10 where the predictions were closer to the experimental data. Furthermore, the difference between the R^2 values and the adjusted R^2 values for biogas yield, methane yield and synergy were not more than 10 %. Also, the low RMSE and the MSE values for biogas yield and synergy show that the model is able to forecast values accurately (Table 6) and this can be attributed to the closeness of the error values to zero which further shows how close the experimental values are to the predicted values.

3.7. Response surface plots

The 3D and 2D response surface plots shown in Figs. 11–13 illustrate the influence of the mixture of feedstocks on biogas yield, methane yield, and synergy respectively. The 3D plots were characterized by different levels of curvature, which corroborates the relationship between substrate mix and biogas yield, methane yield, and synergy and mixture components. The shape of the plot shows that there were notable and shared interactions between HE (A), FLO (B), and KR(C). Both HE and KR had a similar positive synergistic effect on biogas yield, methane yield, and synergy, which was not comparable with that of FLO (Figs. 11–13).

This can also be seen from the coefficients of A and C in the regression model (Equations 16 and 17), i.e., 452.73 and 474.13, as well as 250.47 and 196.17 respectively, for biogas yield and methane yield compared to 375.54 and 138.25 for B. Contextually, increasing the levels of HE and KR in the substrate mix would increase biogas yield, methane yield, and synergy. This observation could be attributed to the fact that HE and KR are rich in nutrients needed for microbial growth, complement each other in buffering the system, and have an optimum C/N ratio. The impact of FLO was not significantly seen. Although FLO could have provided a good carbon source, its insufficient buffer due to low alkalinity levels and its ability to easily degrade and lead to VFA accumulation, pH reduction, and process instability might have led to its less influence. In general, the response surface plots show that the predicted response increases with an increasing HE and KR fractions and decreases with an increasing FLO fraction in the substrate mixtures (Figs. 11–13). This is because the maximum and minimum model outputs were found at the HE-KR and FLO vertices, respectively. This result shows that biogas yield, methane yield, and synergy were more significantly

Affected by the interaction between HE and KR than between FLO and HE and between FLO and KR. Similar observations were

Table 6
RSM performance assessment for biogas yield, methane yield, and synergy.

Parameter	Biogas Yield	Methane Yield	Synergy
R^2	0.999	0.996	0.992
Adjusted R^2	0.997	0.983	0.9681
RMSE	4.798	12.690	0.075
MSE	23.020	161.046	0.006
MAE	3.677	10.559	0.061
MAPE (%)	0.661	4.411	4.774

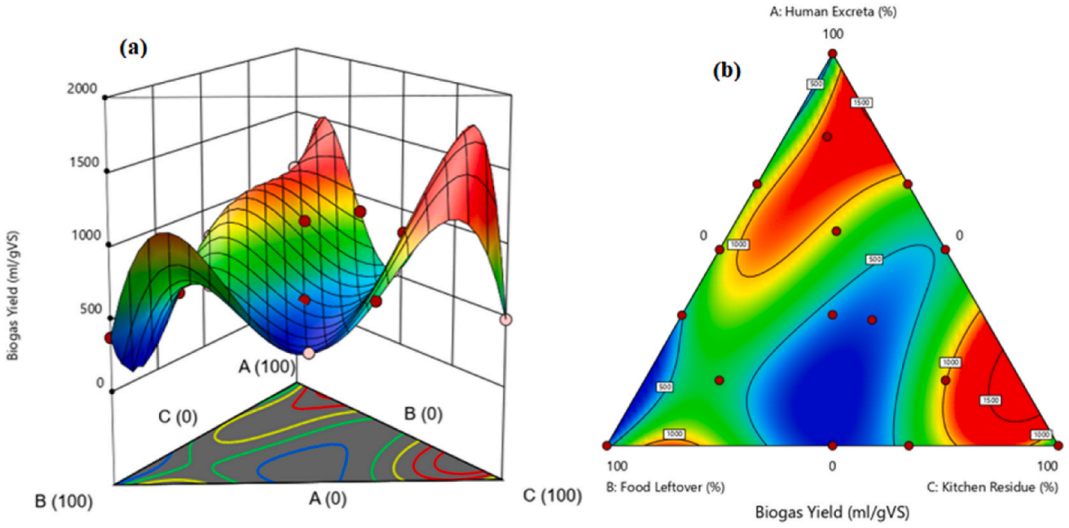

Fig. 11. (a) Three-dimensional and (b)Two-dimensional response surface plots depicting the effect of the substrate mixing ratio on biogas yield. Contour colors represent the levels of model response: blue for low and red for high responses.

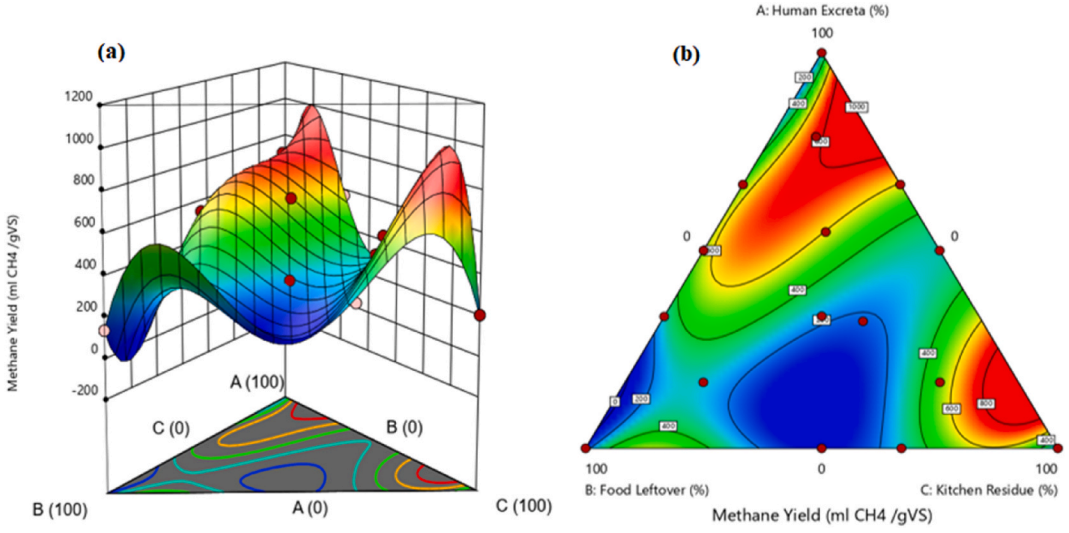

Fig. 12. (a) Three-dimensional and (b)Two-dimensional response surface plots depicting the effect of the substrate mixing ratio on methane yield. Contour colors represent the levels of model response: blue for low and red for high respon

reported by Baek et al. [53], who used a substrate mix of food waste, cattle manure, and pig manure to produce biomethane. The study reported increased methane yield and synergy when food waste and cattle manure was increased but low when pig manure was increased.

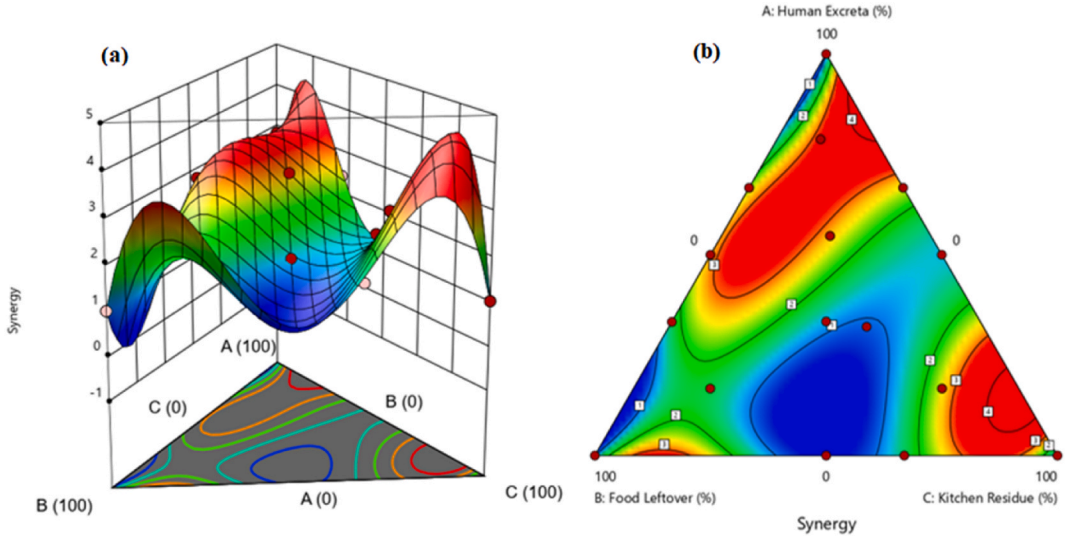

Fig. 13. (a) Three-dimensional and (b)Two-dimensional response surface plots depicting the effect of the substrate mixing ratio on synergy yield. Contour colors represent the levels of model response: blue for low and red for high responses.

4. Conclusions

Ternary substrate mixtures of HE, FLO, and KR formulated for the batch experiment showed that substrate mix R9 (78.8:11.8:9.4) produced the highest amount of methane. R9 (78.8:11.8:9.4) also showed the strongest synergistic effect. The experimental results for the substrate mixtures were used to model the responses of biogas yield, methane yield, and synergistic effects using RSM. The results showed that biogas yield, methane yield, and synergy are significantly influenced by the composition and interactions of feedstock mixtures. Thus, co-digesting substrate mixtures with high amounts of HE and/or KR increased biogas yield, methane yield, and synergy. This finding suggests that it is possible to effectively treat household HE and KR onsite to produce methane for cooking. The 61-day response surface model for synergistic effects predicted an antagonistic effect (SI < 1) only for the co-digestion setting where the FLO fraction is higher than roughly 25 % or the combination of FLO and KR is greater than HE. In order to prevent the potential antagonistic effect, it is recommended to keep the FLO and KR fractions in the substrate combination below 50 %. This study also recommends that in setting up an anaerobic co-digestion system at the household level, the amount of HE should be kept relatively higher (>50 %) than KR and FLO. This is because the higher the amount of HE, the more likely the digestion process would be stable due to the ability of HE to provide a buffering support with its relatively high alkalinity compared to FLO and KR. Also, the high biodegradability of R9 (78.8:11.8:9.4) depicts the ability of the microbial culture to convert the feedstocks in that particular mixing ratio to biogas. Additionally, there is no need to add trace elements to the household biogas system because the household-generated wastes have proven to contain sufficient amounts of trace element such as Zn and Ni that are very beneficial to methanogens.

Funding

This work was supported by the Regional Water and Environmental Sanitation Centre Kumasi (RWESCK) at the Kwame Nkrumah University of Science and Technology (KNUST), Kumasi with funding from the Ghana Government through the World Bank under the Africa Centers of Excellence project.

Data availability statement

Data included in article or supplementary material referenced in article.

CRediT authorship contribution statement

Blissbern Appiagyei Osei-Owusu: Conceptualization, Data curation, Formal analysis, Investigation, Methodology, Project administration, Resources, Software, Validation, Visualization, Writing – original draft. **Richard Arthur:** Conceptualization, Formal analysis, Investigation, Methodology, Resources, Software, Supervision, Validation, Visualization, Writing – review & editing. **Martina Francisca Baidoo:** Conceptualization, Formal analysis, Investigation, Methodology, Resources, Software, Supervision, Validation, Visualization, Writing – review & editing. **Sampson Oduro-Kwarteng:** Conceptualization, Funding acquisition, Investigation, Methodology, Project administration, Resources, Software, Supervision, Validation, Visualization, Writing – review & editing. **Andrew N. Amenaghawon:** Formal analysis, Methodology, Resources, Software, Supervision, Validation, Visualization, Writing –

review & editing.

Declaration of competing interest

The authors declare the following financial interests/personal relationships which may be considered as potential competing interests:Blissbern Appiagyei Osei-Owusu reports financial support was provided by Regional Water and Environmental Sanitation Centre, Kumasi.

References

[1] B. Appiagyei Osei-Owusu, M.F. Baidoo, R. Arthur, S. Oduro-Kwarteng, Physico-chemical characterization of selected feedstocks as co-substrates for household biogas generation in Ghana, Int. J. Sustain. Eng. 16 (1) (2023) 117–128, https://doi.org/10.1080/19397038.2023.2214167.

[2] E. Appiah-Effah, K.B. Nyarko, E. Awuah, Characterization of public toilet sludge from peri-urban and rural areas of Ashanti region of Ghana, J. Appl. Sci. Environ. Sanit. 9 (3) (2014).

[3] R. Arthur, M.F. Baidoo, G. Osei, L. Boamah, S. Kwofie, Evaluation of potential feedstocks for sustainable biogas production in Ghana: quantification, energy generation, and co2 abatement, Cogent Environmental Science 6 (1) (2020) 1868162, https://doi.org/10.1080/23311843.2020.1868162.

[4] D. Ofori-Amanfo, G.N.K. Rockson, A. Arthur, I. Ahmed, Processing dewatered faecal sludge into un pelletized fertilizer for crop production in greater Accra-Ghana, Int. J. Environ. Monit. Anal. 6 (1) (2018) 18–25, https://doi.org/10.11648/j.ijema.20180601.13.

[5] I. Ahmed, D. Ofori-Amanfo, E. Awuah, F. Cobbold, Performance assessment of the rehabilitated mudor sewage treatment plant at James town Accra Ghana, J. Water Resour. Protect. 10 (8) (2018) 725–739, https://doi.org/10.4236/jwarp.2018.108041.

[6] J.K. Nagabooshnam, Solid waste generation and composition in gaborone, Botswana, potential for resource recovery, J. Eng. Technol. Environ. Eng 6 (2011) 4878–4884.

[7] K. Miezah, K. Obiri-Danso, Z. Kádár, B. Fei-Baffoe, M.Y. Mensah, Municipal solid waste characterization and quantification as a measure towards effective waste management in Ghana, Waste Manag. 46 (2015) 15–27, https://doi.org/10.1016/j.wasman.2015.09.009.

[8] E.M. Abalo, P. Peprah, J. Nyonyo, R. Ampomah-Sarpong, W. Agyemang-Duah, A review of the triple gains of waste and the way forward for Ghana, Journal of Renewable Energy (2018), https://doi.org/10.1155/2018/9737683.

[9] J. Kim, J. Kim, C. Lee, Anaerobic co-digestion of food waste, human feces, and toilet paper: methane potential and synergistic effect, Fuel 248 (2019) 189–195, https://doi.org/10.1016/j.fuel.2019.03.081.

[10] R. Kyere, M. Addaney, J.A. Akudugu, Decentralization and solid waste management in urbanizing Ghana: moving beyond the status quo, in: Municipal Solid Waste Management, IntechOpen, 2019.

[11] T. Elmitwalli, M. Van Leeuwen, K. Kujawa-Roeleveld, W. Sanders, G. Zeeman, Anaerobic biodegradability and digestion in accumulation systems for concentrated black water and kitchen organic-wastes, Water Sci. Technol. 53 (8) (2006) 167–175, https://doi.org/10.2166/wst.2006.247.

[12] M. Fajobi, O. Lasode, A. Adeleke, P. Ikubanni, A. Balogun, Investigation of physicochemical characteristics of selected lignocellulose biomass, Sci. Rep. 12 (1) (2022) 1–14, https://doi.org/10.1038/s41598-022-07061-2.

[13] M. Pöschl, S. Ward, P. Owende, Evaluation of energy efficiency of various biogas production and utilization pathways, Appl. Energy 87 (11) (2010) 3305–3321, https://doi.org/10.1016/j.apenergy.2010.05.011.

[14] S. Khoufi, A. Louhichi, S. Sayadi, Optimization of anaerobic codigestion of olive mill wastewater and liquid poultry manure in batch condition and semi-continuous jet-loop reactor, Bioresour. Technol. 182 (2015) 67–74, https://doi.org/10.1016/j.biortech.2015.01.092.

[15] G.K. Kafle, S.H. Kim, K.I. Sung, Batch anaerobic co-digestion of kimchi factory waste silage and swine manure under mesophilic conditions, Bioresour. Technol. 124 (2012) 489–494, https://doi.org/10.1016/j.biortech.2012.08.066.

[16] C. Rico, N. Muñoz, J. Fernández, J.L. Rico, High-load anaerobic codigestion of cheese whey and liquid fraction of dairy manure in a one-stage uasb process: limits in co-substrates ratio and organic loading rate, Chem. Eng. J. 262 (2015) 794–802, https://doi.org/10.1016/j.cej.2014.10.050.

[17] X. Ma, M. Yu, M. Yang, M. Gao, C. Wu, Q. Wang, Synergistic effect from anaerobic co-digestion of food waste and sophora flavescens residues at different co-substrate ratios, Environ. Sci. Pollut. Control Ser. 26 (36) (2019) 37114–37124, https://doi.org/10.1007/s11356-019-06399-x.

[18] S.L. Chiu, I. Lo, Reviewing the anaerobic digestion and co-digestion process of food waste from the perspectives on biogas production performance and environmental impacts, Environ. Sci. Pollut. Control Ser. 23 (24) (2016) 24435–24450, https://doi.org/10.1007/s11356-016-7159-2.

[19] J. Mata-Alvarez, J. Dosta, M. Romero-Güiza, X. Fonoll, M. Peces, S. Astals, A critical review on anaerobic co-digestion achievements between 2010 and 2013, Renew. Sustain. Energy Rev. 36 (2014) 412–427, https://doi.org/10.1016/j.rser.2014.04.039.

[20] J. Mata-Alvarez, S. Macé, P. Llabres, Anaerobic digestion of organic solid wastes. an overview of research achievements and perspectives, Bioresour. Technol. 74 (1) (2000) 3–16, https://doi.org/10.1016/S0960-8524(00)00023-7.

[21] F.J. Andriamanohiarisoamanana, A. Saikawa, T. Kan, G. Qi, Z. Pan, T. Yamashiro, M. Iwasaki, I. Ihara, T. Nishida, K. Umetsu, Semi-continuous anaerobic co-digestion of dairy manure, meat and bone meal and crude glycerol: process performance and digestate valorization, Renew. Energy 128 (2018) 1–8, https://doi.org/10.1016/j.renene.2018.05.056.

[22] F.J. Andriamanohiarisoamanana, A. Saikawa, K. Tarukawa, G. Qi, Z. Pan, T. Yamashiro, M. Iwasaki, I. Ihara, T. Nishida, K. Umetsu, Anaerobic co-digestion of dairy manure, meat and bone meal, and crude glycerol under mesophilic conditions: synergistic effect and kinetic studies, Energy for Sustainable Development 40 (2017) 11–18, https://doi.org/10.1016/j.esd.2017.05.008.

[23] V. Moset, D. Fontaine, H.B. Møller, Co-digestion of cattle manure and grass harvested with different technologies. effect on methane yield, digestate composition and energy balance, Energy 141 (2017) 451–460, https://doi.org/10.1016/j.energy.2017.08.068.

[24] S. Astals, R. Musenze, X. Bai, S. Tannock, S. Tait, S. Pratt, P. Jensen, Anaerobic co-digestion of pig manure and algae: impact of intracellular algal products recovery on co-digestion performance, Bioresour. Technol. 181 (2015) 97–104, https://doi.org/10.1016/j.biortech.2015.01.039.

[25] K. Hagos, J. Zong, D. Li, C. Liu, X. Lu, Anaerobic co-digestion process for biogas production: progress, challenges and perspectives, Renew. Sustain. Energy Rev. 76 (2017) 1485–1496, https://doi.org/10.1016/j.rser.2016.11.184.

[26] J. Filer, H.H. Ding, S. Chang, Biochemical methane potential (bmp) assay method for anaerobic digestion research, Water 11 (5) (2019) 921, https://doi.org/10.3390/w11050921.

[27] K. Koch, S.D. Hafner, S. Weinrich, S. Astals, Identification of critical problems in biochemical methane potential (bmp) tests from methane production curves, Front. Environ. Sci. (2019) 178, https://doi.org/10.3389/fenvs.2019.00178.

[28] C. Holliger, M. Alves, D. Andrade, I. Angelidaki, S. Astals, U. Baier, C. Bougrier, P. Buffière, M. Carballa, V. De Wilde, et al., Towards a standardization of biomethane potential tests, Water Sci. Technol. 74 (11) (2016) 2515–2522, https://doi.org/10.2166/wst.2016.336.

[29] F. Raposo, V. Fernández-Cegrí, M. De la Rubia, R. Borja, F. Béline, C. Cavinato, G. Demirer, B. Fernández, M. Fernández-Polanco, J. Frigon, et al., Biochemical methane potential (bmp) of solid organic substrates: evaluation of anaerobic biodegradability using data from an international interlaboratory study, J. Chem. Technol. Biotechnol. 86 (8) (2011) 1088–1098, https://doi.org/10.1002/jctb.2622.

[30] I. Angelidaki, M. Alves, D. Bolzonella, L. Borzacconi, J. Campos, A. Guwy, S. Kalyuzhnyi, P. Jenicek, J. Van Lier, Defining the biomethane potential (bmp) of solid organic wastes and energy crops: a proposed protocol for batch assays, Water Sci. Technol. 59 (5) (2009) 927–934, https://doi.org/10.2166/wst.2009.040.

[31] F.M. Hussien, A.J. Hamad, J.J. Faraj, Impact of adding cow dung with different ratios on anaerobic co-digestion of waste food for biogas production, J. Mech. Eng. Res. Dev 43 (7) (2020) 213–221, https://doi.org/10.13140/RG.2.2.14821.63209.

[32] K. Paritosh, S.K. Kushwaha, M. Yadav, N. Pareek, A. Chawade, V. Vivekanand, Food waste to energy: an overview of sustainable approaches for food waste management and nutrient recycling, BioMed Res. Int. 2017 (2017), https://doi.org/10.1155/2017/2370927.
[33] American Public Health Association (Apha), Standard Methods for the Examination of Water and Wastewater 20th Edition, American Public Health Association, American Water Work Association, Water Environment Federation, Washington, DC, 1998.
[34] J. Bremner, Total nitrogen, Methods of soil analysis: part 2 chemical and microbiological properties 9 (1965) 1149–1178, https://doi.org/10.2134/agronmonogr9.2.c32.
[35] D. Singh, P. Chhonkar, R. Pandey, Soil Plant Water Analysis: a Methods Manual, IARI, New Delhi, 1999, pp. 80–82.
[36] E. McLean, Aluminum, Methods of Soil Analysis: Part 2 Chemical and Microbiological Properties 9 (1965) 978–998.
[37] D. Heanes, Determination of total organic-c in soils by an improved chromic acid digestion and spectrophotometric procedure, Commun. Soil Sci. Plant Anal. 15 (10) (1984) 1191–1213, https://doi.org/10.1080/00103628409367551.
[38] D.W. Nelson, Total Carbon, Organic, and Organic Matter, Chemical and microbiological properties, 1982, pp. 539–577.
[39] S. Dahunsi, C. Osueke, T. Olayanju, A. Lawal, Co-digestion of Theobroma cacao (cocoa) pod husk and poultry manure for energy generation: effects of pretreatment methods, Bioresour. Technol. 283 (2019) 229–241, https://doi.org/10.1016/j.biortech.2019.03.093.
[40] P.K. Singh, H. Srichandan, S.K. Ojha, R. Pattnaik, S.K. Verma, S. Pal, J. Singh, S. Mishra, Evaluation of Biomethane Potential of Codigested Sheep Manure and Kitchen Refuse, Biomass Conversion and Biorefinery, 2021, pp. 1–11, https://doi.org/10.1007/s13399-021-01961-5.
[41] P.K. Singh, H. Srichandan, S.K. Ojha, S. Mishra, K. Naik, A comparative study of biogasification of wheat straw, sugarcane bagasse and pressmud, Journal of Environmental Science and Health, Part A 54 (4) (2019) 306–314, https://doi.org/10.1080/10934529.2018.1548812.
[42] P.K. Singh, S.K. Verma, S.K. Ojha, P.K. Panda, H. Srichandan, E. Jha, S. Mishra, Intrinsic molecular insights to enhancement of biogas production from kitchen refuse using alkaline-microwave pretreatment, Sci. Rep. 9 (1) (2019) 1–12, https://doi.org/10.1038/s41598-019-42471-9.
[43] W. Boyle, Energy recovery from sanitary landfills-a review, Microbial energy conversion (1976) 119–138, https://doi.org/10.1016/b978-0-08-021791-8.50019-6.
[44] P.A. Scherer, R. Arthur, S. Antonczyk, Accelerated biomethane potential assay for straw with artificially flocculated sludge and defined 'synthetic manure', Bioresour. Technol. Rep. 15 (2021) 100787 https://doi.org/10.1016/j.biteb.2021.100787.
[45] F. Steffen, A. Requejo, C. Ewald, R. Janzon, B. Saake, Anaerobic digestion of fines from recovered paper processing–influence of fiber source, lignin and ash content on biogas potential, Bioresour. Technol. 200 (2016) 506–513, https://doi.org/10.1016/j.biortech.2015.10.014.
[46] M.O. Fagbohungbe, B.M. Herbert, H. Li, L. Ricketts, K.T. Semple, The effect of substrate to inoculum ratios on the anaerobic digestion of human faecal material, Environ. Technol. Innovat. 3 (2015) 121–129, https://doi.org/10.1016/j.eti.2015.02.005.
[47] F. Raposo, R. Borja, J. Cacho, J. Mumme, K. Orupõld, S. Esteves, J. Noguerol-Arias, S. Picard, A. Nielfa, P. Scherer, et al., First international comparative study of volatile fatty acids in aqueous samples by chromatographic techniques: evaluating sources of error, TrAC, Trends Anal. Chem. 51 (2013) 127–143, https://doi.org/10.1016/j.trac.2013.07.007.
[48] W.F. Owen, D.C. Stuckey, J.B. Healy Jr., L.Y. Young, P.L. McCarty, Bioassay for monitoring biochemical methane potential and anaerobic toxicity, Water Res. 13 (6) (1979) 485–492, https://doi.org/10.1016/0043-1354(79)90043-5.
[49] VDI, VDI 4630: Fermentation of Organic Materials: Characterisation of the Substrate, Sampling, Collection of Material Data, Fermentation Tests, Beuth Verlag, 2016, p. 4630.
[50] B. Wang, I.A. Nges, M. Nistor, J. Liu, Determination of methane yield of cellulose using different experimental setups, Water Sci. Technol. 70 (4) (2014) 599–604, https://doi.org/10.2166/wst.2014.275.
[51] T. Hou, J. Zhao, Z. Lei, K. Shimizu, Z. Zhang, Synergistic effects of rice straw and rice bran on enhanced methane production and process stability of anaerobic digestion of food waste, Bioresour. Technol. 314 (2020) 123775, https://doi.org/10.1016/j.biortech.2020.123775.
[52] J.H. Ebner, R.A. Labatut, J.S. Lodge, A.A. Williamson, T.A. Trabold, Anaerobic co-digestion of commercial food waste and dairy manure: characterizing biochemical parameters and synergistic effects, Waste Manag. 52 (2016) 286–294, https://doi.org/10.1016/j.wasman.2016.03.046.
[53] G. Baek, D. Kim, J. Kim, H. Kim, C. Lee, Treatment of cattle manure by anaerobic co-digestion with food waste and pig manure: methane yield and synergistic effect, Int. J. Environ. Res. Publ. Health 17 (13) (2020) 4737, https://doi.org/10.3390/ijerph17134737.
[54] G. Capson-Tojo, M. Rouez, M. Crest, E. Trably, J.-P. Steyer, N. Bernet, J.-P. Delgenès, R. Escudié, Kinetic study of dry anaerobic co-digestion of food waste and cardboard for methane production, Waste Manag. 69 (2017) 470–479, https://doi.org/10.1016/j.wasman.2017.09.002.
[55] Y. Li, R. Zhang, X. Liu, C. Chen, X. Xiao, L. Feng, Y. He, G. Liu, Evaluating methane production from anaerobic mono-and co-digestion of kitchen waste, corn stover, and chicken manure, Energy Fuels 27 (4) (2013) 2085–2091, https://doi.org/10.1021/ef400117f.
[56] L. Neves, R. Oliveira, M. Alves, Co-digestion of cow manure, food waste and intermittent input of fat, Bioresour. Technol. 100 (6) (2009) 1957–1962, https://doi.org/10.1016/j.biortech.2008.10.030.
[57] A.J. Ward, P.J. Hobbs, P.J. Holliman, D.L. Jones, Optimisation of the anaerobic digestion of agricultural resources, Bioresour. Technol. 99 (17) (2008) 7928–7940, https://doi.org/10.1016/j.biortech.2008.02.044.
[58] S.K. Pramanik, F.B. Suja, M. Porhemmat, B.K. Pramanik, Performance and kinetic model of a single-stage anaerobic digestion system operated at different successive operating stages for the treatment of food waste, Processes 7 (9) (2019) 600, https://doi.org/10.3390/pr7090600.
[59] R. Dar, M. Parmar, E. Dar, R. Sani, U. Phutela, Biomethanation of agricultural residues: potential, limitations and possible solutions, Renew. Sustain. Energy Rev. 135 (2021) 110217, https://doi.org/10.1016/j.rser.2020.110217.
[60] M.A. Rahman, H.B. Møller, C.K. Saha, M.M. Alam, R. Wahid, L. Feng, Optimal ratio for anaerobic co-digestion of poultry droppings and lignocellulosic-rich substrates for enhanced biogas production, Energy for Sustainable Development 39 (2017) 59–66, https://doi.org/10.1016/j.esd.2017.04.004.
[61] M.R. Haider, S. Yousaf, R.N. Malik, C. Visvanathan, et al., Effect of mixing ratio of food waste and rice husk co-digestion and substrate to inoculum ratio on biogas production, Bioresour. Technol. 190 (2015) 451–457, https://doi.org/10.1016/j.biortech.2015.02.105.
[62] S. Singh, N. Hariteja, S. Sharma, N.J. Raju, T.R. Prasad, Production of biogas from human faeces mixed with the co-substrate poultry litter & cow dung, Environ. Technol. Innovat. 23 (2021) 101551, https://doi.org/10.1016/j.eti.2021.101551.
[63] M. Rouf, P. Bajpai, C. Jotshi, Optimization of biogas generation from press mud in batch reactor, Bangladesh J. Sci. Ind. Res. 45 (4) (2010) 371–376, https://doi.org/10.3329/bjsir.v45i4.7383.
[64] J. Lin, J. Zuo, L. Gan, P. Li, F. Liu, K. Wang, L. Chen, H. Gan, Effects of mixture ratio on anaerobic co-digestion with fruit and vegetable waste and food waste of China, J. Environ. Sci. 23 (8) (2011) 1403–1408, https://doi.org/10.1016/S1001-0742(10)60572-4.
[65] T. Hou, N. Chen, S. Tong, B. Li, Q. He, C. Feng, Enhancement of rice bran as carbon and microbial sources on the nitrate removal from groundwater, Biochem. Eng. J. 148 (2019) 185–194, https://doi.org/10.1016/j.bej.2018.07.010.
[66] G. Capson-Tojo, M. Rouez, M. Crest, J.-P. Steyer, J.-P. Delgenès, R. Escudié, Food waste valorization via anaerobic processes: a review, Rev. Environ. Sci. Biotechnol. 15 (3) (2016) 499–547, https://doi.org/10.1007/s11157-016-9405-y.
[67] R. Arthur, P.A. Scherer, Monitoring dissolved active trace elements in biogas plants using total reflection x-ray fluorescence spectrometry, X Ray Spectrom. 49 (5) (2020) 560–571, https://doi.org/10.1002/xrs.3151.
[68] X. Huang, S. Yun, J. Zhu, T. Du, C. Zhang, X. Li, Mesophilic anaerobic co-digestion of aloe peel waste with dairy manure in the batch digester: focusing on mixing ratios and digestate stability, Bioresour. Technol. 218 (2016) 62–68, https://doi.org/10.1016/j.biortech.2016.06.070.
[69] M.R. Miah, A.K.M.L. Rahman, M.R. Akanda, A. Pulak, M.A. Rouf, Production of biogas from poultry litter mixed with the co-substrate cow dung, J. Taibah Univ. Sci. 10 (4) (2016) 497–504, https://doi.org/10.1016/j.jtusci.2015.07.007.
[70] B. Abubakar, N. Ismail, Anaerobic digestion of cow dung for biogas production, ARPN J. Eng. Appl. Sci. 7 (2) (2012) 169–172.
[71] P. Scherer, Operating analytics of biogas plants to improve efficiency and to ensure process stability, Progress in Biogas Stuttgart-Hohenheim (2007) 77–84.
[72] L. Feng, Y. Li, C. Chen, X. Liu, X. Xiao, X. Ma, R. Zhang, Y. He, G. Liu, Biochemical methane potential (bmp) of vinegar residue and the influence of feed to inoculum ratios on biogas production, Bioresources 8 (2) (2013) 2487–2498, https://doi.org/10.15376/biores.8.2.2487-2498.

[73] P. Worm, F.G. Fermoso, P.N. Lens, C.M. Plugge, Decreased activity of a propionate degrading community in a uasb reactor fed with synthetic medium without molybdenum, tungsten and selenium, Enzym. Microb. Technol. 45 (2) (2009) 139–145, https://doi.org/10.1016/j.enzmictec.2009.02.001.
[74] P. Gikas, Kinetic responses of activated sludge to individual and joint nickel (ni (ii)) and cobalt (co (ii)): an isobolographic approach, J. Hazard Mater. 143 (1–2) (2007) 246–256, https://doi.org/10.1016/j.jhazmat.2006.09.019.
[75] C. Li, H.H. Fang, Inhibition of heavy metals on fermentative hydrogen production by granular sludge, Chemosphere 67 (4) (2007) 668–673, https://doi.org/10.1016/j.chemosphere.2006.11.005.
[76] M.T. Agler, M.L. Garcia, E.S. Lee, M. Schlicher, L.T. Angenent, Thermophilic anaerobic digestion to increase the net energy balance of corn grain ethanol, Environ. Sci. Technol. 42 (17) (2008) 6723–6729, https://doi.org/10.1021/es800671a.
[77] D.H. Zitomer, C.C. Johnson, R.E. Speece, Metal stimulation and municipal digester thermophilic/mesophilic activity, J. Environ. Eng. 134 (1) (2008) 42–47, https://doi.org/10.1061/(ASCE)0733-9372(2008)134:1(42).
[78] R. Arthur, S. Antonczyk, S. Off, P.A. Scherer, Mesophilic and thermophilic anaerobic digestion of wheat straw in a cstr system with 'synthetic manure': impact of nickel and tungsten on methane yields, cell count, and microbiome, Bioengineering 9 (1) (2022) 13, https://doi.org/10.3390/bioengineering9010013.
[79] T. Schmidt, M. Nelles, F. Scholwin, J. Pröter, Trace element supplementation in the biogas production from wheat stillage–optimization of metal dosing, Bioresour. Technol. 168 (2014) 80–85, https://doi.org/10.1016/j.biortech.2014.02.124.
[80] F.G. Fermoso, J. Bartacek, S. Jansen, P.N. Lens, Metal supplementation to uasb bioreactors: from cell-metal interactions to full-scale application, Sci. Total Environ. 407 (12) (2009) 3652–3667, https://doi.org/10.1016/j.scitotenv.2008.10.043.
[81] P. Schönheit, J. Moll, R.K. Thauer, Nickel, cobalt, and molybdenum requirement for growth of methanobacterium thermoautotrophicum, Arch. Microbiol. 123 (1) (1979) 105–107, https://doi.org/10.1007/bf00403508.
[82] Y. Wang, G. Li, M. Chi, Y. Sun, J. Zhang, S. Jiang, Z. Cui, Effects of co-digestion of cucumber residues to corn stover and pig manure ratio on methane production in solid state anaerobic digestion, Bioresour. Technol. 250 (2018) 328–336, https://doi.org/10.1016/j.biortech.2017.11.055.
[83] B. Dan-Asabe, S. Yaro, D. Yawas, S. Aku, Statistical modeling and optimization of the flexural strength, water absorption and density of a doum palmkankara clay filler hybrid composite, Journal of King Saud University-Engineering Sciences 31 (4) (2019) 385–394, https://doi.org/10.1016/j.jksues.2017.11.003.
[84] A.N. Amenaghawon, P.I. Orukpe, J. Nwanbi-Victor, M.O. Okedi, E.I. Aburime, Enhanced lipase production from a ternary substrate mix of agricultural residues: a case of optimization of microbial inducers and global sensitivity analysis, Bioresour. Technol. Rep. 17 (2022) 101000, https://doi.org/10.1016/j.biteb.2022.101000.
[85] E. Betiku, O.A. Adesina, Statistical approach to the optimization of citric acid production using filamentous fungus aspergillus Niger grown on sweet potato starch hydrolyzate, Biomass Bioenergy 55 (2013) 350–354, https://doi.org/10.1016/j.biombioe.2013.02.034.
[86] H. Le Man, S. Behera, H. Park, Optimization of operational parameters for ethanol production from Korean food waste leachate, Int. J. Environ. Sci. Technol. 7 (2010) 157–164, https://doi.org/10.1007/bf03326127.
[87] A. Koocheki, A.R. Taherian, S.M. Razavi, A. Bostan, Response surface methodology for optimization of extraction yield, viscosity, hue and emulsion stability of mucilage extracted from lepidium perfoliatum seeds, Food Hydrocolloids 23 (8) (2009) 2369–2379, https://doi.org/10.1016/j.foodhyd.2009.06.014.
[88] O.B. Osunkanmibi, T.O. Owolabi, E. Betiku, Comparison of artificial neural network and response surface methodology performance on fermentation parameters optimization of bioconversion of cashew apple juice to gluconic acid, Int. J. Food Eng. 11 (3) (2015) 393–403, https://doi.org/10.1515/ijfe-2015-0072.